UNIVERSIDADE FEDERAL DO CEARÁ

CENTRO DE CIÊNCIAS

DEPARTAMENTO DE BIOQUÍMICA E BIOLOGIA MOLECULAR

PROGRAMA DE PÓS-GRADUAÇÃO EM BIOQUÍMICA

TIAGO DEIVESON PEREIRA LOPES

CARACTERIZAÇÃO ESTRUTURAL E AÇÃO CICATRIZANTE DE UMA PROTEÍNA LIGANTE À QUITINA DE SEMENTES DE *Moringa oleifera* COM ATIVIDADE ANTI-INFLAMATÓRIA

FORTALEZA

2022

TIAGO DEIVESON PEREIRA LOPES

CARACTERIZAÇÃO ESTRUTURAL E AÇÃO CICATRIZANTE DE UMA PROTEÍNA LIGANTE À QUITINA DE SEMENTES DE *Moringa oleifera* COM ATIVIDADE ANTI-INFLAMATÓRIA

Tese apresentada ao Programa de Pós-Graduação em Bioquímica e Biologia Molecular da Universidade Federal do Ceará, como requisito para a obtenção do título de Doutor em Bioquímica. Área de concentração: Bioquímica Vegetal

Orientadora: Profª. Drª. Daniele de Oliveira Bezerra de Sousa
Co-orientadora: Profª. Drª. Nylane Maria Nunes de Alencar

FORTALEZA

2022

Dados Internacionais de Catalogação na Publicação
Universidade Federal do Ceará
Sistema de Bibliotecas
Gerada automaticamente pelo módulo Catalog, mediante os dados fornecidos pelo(a) autor(a)

L856c Lopes, Tiago Deiveson Pereira.
Caracterização estrutural e ação cicatrizante de uma proteína ligante à quitina de sementes de Moringa oleifera com atividade anti-inflamatória / Tiago Deiveson Pereira Lopes. – 2022.
90 f. : il. color.

Tese (doutorado) – Universidade Federal do Ceará, Centro de Ciências, Programa de Pós-Graduação em Bioquímica , Fortaleza, 2022.
Orientação: Profa. Dra. Daniele de Oliveira Bezerra de Sousa.
Coorientação: Profa. Dra. Nylane Maria Nunes de Alencar.

1. Lectinas. 2. Moringa oleifera. 3. estrutura tridimensional. 4. processo cicatricial. I. Título.

CDD 572

TIAGO DEIVESON PEREIRA LOPES

CARACTERIZAÇÃO ESTRUTURAL E AÇÃO CICATRIZANTE DE UMA PROTEÍNA LIGANTE À QUITINA DE SEMENTES DE *Moringa oleifera* COM ATIVIDADE ANTI-INFLAMATÓRIA

Tese apresentada ao Programa de Pós-Graduação em Bioquímica e Biologia Molecular da Universidade Federal do Ceará, como requisito para a obtenção do título de Doutor em Bioquímica. Área de concentração: Bioquímica Vegetal

Aprovada em: 25/04/2022

BANCA EXAMINADORA

_____

Profª. Drª. Daniele de Oliveira Bezerra de Sousa
Universidade Federal do Ceará (Orientadora)

_____

Profª. Drª. Nylane Maria Nunes de Alencar
Universidade Federal do Ceará (Co-orientadora)

_____

Prof. Dr. Bruno Anderson Matias da Rocha
Universidade Federal do Ceará

_____

Prof. Dr. Claudener Souza Teixeira
Universidade Federal do Cariri

_____

Profª. Drª. Maria Izabel Florindo Guedes
Universidade Estadual do Ceará

RESUMO

Lectinas são definidas como proteínas que possuem a capacidade de se ligar de forma especifica a carboidratos sem, contudo, alterar suas estruturas químicas. Devido as diversas atividades biológicas apresentadas por essas proteínas, elas vêm ganhando uma enorme importância no ramo da Biotecnologia e grande parte dessas atividades está diretamente relacionada com o domínio de interação a carboidratos. Atualmente, é cada vez maior o número de estudos com foco na determinação da estrutura tridimensional das lectinas visando elucidar os mecanismos de ação envolvidos em tais atividades. Nesse contexto, o presente projeto propõe estudar os mecanismos de ação envolvidos na atividade anti-inflamatória apresentada por *Mo*-CBP$_4$, uma lectina ligante à quitina isolada de sementes de *Moringa oleifera*. Para tanto, serão obtidas as estruturas primária e tridimensional da lectina através das técnicas de espectrometria de massas e cristalografia de raios-X para posterior análise *in silico* da interação com seus ligantes. Além de propor a investigação dos efeitos de *Mo*-CBP$_4$ sobre o processo cicatricial de feridas cutâneas através da utilização de modelos experimentais de feridas cutâneas em camundongos e utilização de cultura de células. Como perspectivas, é esperado que os resultados obtidos nesse projeto possam contribuir para uma melhor compreensão acerca da estrutura tridimensional de *Mo*-CBP$_4$ e a relação com sua atividade anti-inflamatória. Além disso, contribuir para um fornecimento de informações sobre o uso dessa lectina como potencial agente cicatrizante.

Palavras-chave: Lectinas; *Moringa oleifera*; estrutura tridimensional; processo cicatricial.

ABSTRACT

Lectins are defined as proteins that have the ability to specifically bind carbohydrates without, however, changing their chemical structures. Due to the diverse biological activities presented by these proteins, they have been gaining enormous importance in the field of Biotechnology and most of these activities are directly related to the domain of interaction with carbohydrates. Currently, there is an increasing number of studies focusing on the determination of the three-dimensional structure of lectins in order to elucidate the mechanisms of action involved in such activities. In this context, the present project proposes to study the mechanisms of action involved in the anti-inflammatory activity presented by *Mo*-CBP$_4$, a chitin-binding lectin isolated from *Moringa oleifera* seeds. Therefore, the primary and three-dimensional structures of the lectin will be obtained through mass spectrometry and X-ray crystallography techniques for further in silico analysis of the interaction with its ligands. In addition to proposing the investigation of the effects of *Mo*-CBP$_4$ on the healing process of skin wounds through the use of experimental models of skin wounds in mice and the use of cell culture. As perspectives, it is expected that the results obtained in this project can contribute to a better understanding of the three-dimensional structure of *Mo*-CBP$_4$ and the relationship with its anti-inflammatory activity. In addition, to contribute to the provision of information on the use of this lectin as a potential healing agent.

Keywords: Lectins; *Moringa oleifera*; three-dimensional structure; healing process.

LISTA DE FIGURAS

LISTA DE TABELAS

LISTA DE ABREVIATURAS E SIGLAS

ANOVA	Análise de Variância
ATCC	American Type Culture Collection
BLAST	Basic Local Alignment Search Tool
BSA	Bovine Serum Albumin
CCP4	Collaborative Computacional Project Number 4
Cg	Carragenina
CM	Carboximetil
DMEM	Dulbecco's Modified Eagle Medium
DRC	Domínio de Reconhecimento a Carboidrato
ELISA	Enzyme Linked Immuno Sorbent Assay
ESI-TOF	Electrospray Ionization Time-of-Flight
GlycNac	N-acetil-D-glucosamina
HPLC	High-Performance Liquid Chromatography
IL	Interleucina
IP	Intraperitoneal
IU	International Unit
Mo-CBP	*Moringa oleifera* – Chitin Binding Protein
MPO	Myeloperoxidase
MS	Mass Spectrometry
NCBI	National Center of Biotechnology Information
PBS	Phosphate-Buffered Saline
PDB	Protein Data Bank

PO	Per Oral
PVA	Polyvinyl Alcohol
SEM	Standard Error of the Mean
SRB	Sulforodamine B
TGF-β	Transforming Growth Factor beta
TNF-α	Tumor Necrosis Factor alpha
UPLC	Ultra Performance Liquid Chromatography
VEGF	Vascular Endothelial Growth Factor
Zy	Zymosan

SUMÁRIO

1 INTRODUÇÃO

As lectinas são definidas como proteínas ou glicoproteínas de origem não imune e que são capazes de reconhecer e se ligar, de forma reversível, a mono ou oligossacarídeos específicos sem, contudo, alterar suas estruturas químicas. Essas moléculas são ubíquas, com ampla distribuição na natureza, tendo sido encontradas em vírus, bactérias, fungos, algas, vegetais superiores, invertebrados e vertebrados (PEUMANS; VAN DAMME, 1995; GHAZARIAN *et al.,* 2011). Entretanto, devido sua facilidade de isolamento e importância econômica e nutricional, as lectinas de plantas são as mais bem estudadas (LIS; SHARON, 1998).

Nos últimos anos, as lectinas de plantas têm ganhado uma enorme importância no ramo da Biotecnologia e grande parte dessa importância depende da interação da lectina com algum componente glicosídico. As lectinas já foram relatadas exercendo as mais variadas atividades: atividade inseticida (ROY *et al.,* 2014), atividade antifúngica (CHARUNGCHITRAK *et al.,* 2011; KLAFKE *et al.,* 2013), atividade bactericida (CARVALHO *et al.,* 2015), atividade antitumoral (LIU *et al.,* 2013), atividade anti-inflamatória (ALENCAR *et al.,* 1999; SANTI-GADELHA *et al.,* 2006; MOTA *et al*., 2006) e cicatrizante (BEZERRA, 2015).

Visando elucidar os mecanismos de ação envolvidos nessas atividades biológicas das lectinas é que tem aumentado bastante o número de pesquisas com foco na determinação da estrutura tridimensional dessas proteínas. Atualmente, várias lectinas já tiveram suas estruturas primárias e terciárias determinadas, o que tem fornecido inúmeros dados bioquímicos sobre suas interações com seus respectivos ligantes e consequentemente uma maior compreensão acerca de suas propriedades biológicas (SINGH; SARATHI, 2012; BEZERRA *et al.,* 2013; DELATORRE *et al.,* 2013; SOUSA *et al.,* 2015).

A partir da farinha de sementes da espécie *Moringa oleifera* Lamarck, uma espécie originária do norte da Índia, foi isolada, por nosso grupo de pesquisa, uma lectina ligante à quitina com atividade antimicrobiana, antinociceptiva e anti-inflamatória, denominada *Mo*-CBP$_4$ (*Mo*: *M. oleifera*, CBP: “Chitin Binding Protein” e a numeração indica a ordem de eluição da proteína na matriz CM-Sepharose). *Mo*-CBP$_4$ mostrou atividade antifúngica e apresentou potentes atividades antinociceptiva e anti-inflamatória, quando administrada em camundongos por via oral. A proteína, quando incubada com seu carboidrato específico, o N-acetil-D-glucosamina (GlycNac), teve

sua atividade anti-inflamatória totalmente revertida (PEREIRA *et al*., 2011; PEREIRA, 2014; LOPES, 2016). Isso sugere que o sítio lectínico de *Mo*-CBP$_4$ está diretamente envolvido no mecanismo de ação anti-inflamatório. Portanto, mais estudos são necessários para investigar o papel da interação ao carboidrato na atividade biológica citada, principalmente estudos voltados para a determinação da composição e estrutura tridimensional da proteína. *Mo*-CBP$_4$ caracteriza-se ainda por possuir massa molecular de 12,0 KDa e tratar-se de uma glicoproteína com 2,9% de carboidrato e pI de 10,55. *Mo*-CBP$_4$ mostrou-se altamente estável ao calor, mantendo sua atividade anti-inflamatória inalterada após tratamento térmico (100 °C) por 1 hora (PEREIRA *et al.,* 2011*,* PEREIRA, 2014).

As propriedades antimicrobianas e anti-inflamatórias citadas de *Mo*-CBP$_4$ suscitam seu potencial para aplicação como um provável agente cicatrizante, tendo em vista que essas atividades estão entre as principais responsáveis pela restauração de tecidos lesionados (SÜNTAR *et al.,* 2011; THAKUR *et al*., 2011; YARISWAMY *et al*., 2013). Por sua vez, a atividade anti-inflamatória é a mais associada à existência de uma potencial ação cicatrizante, sendo tal fato comprovado por relatos, na literatura, de lectinas exercerem atividade cicatrizante através da modulação de fatores inflamatórios essenciais para a regulação do processo cicatricial (CORIOLANO *et al.,* 2014; BEZERRA, 2015). Além disso, a própria espécie da qual *Mo*-CBP$_4$ foi isolada possui um histórico já relatado de atividade cicatrizante (CHOPRA, 1993; RAWAT *et al.,* 2012; BHATNAGAR *et al.,* 2013; SIVARANJANI; PHILOMINATHAN, 2016).

Então, diante de um contexto marcado pelo grande número de pessoas com feridas cutâneas crônicas, devido, principalmente, à ineficiência dos tratamentos existentes, e pelo avanço da utilização de agentes de origem vegetal no tratamento e manejo de feridas, devido a redução do tempo de reparo e risco de complicações infecciosas, *Mo*-CBP$_4$ apresenta-se como uma promissora alternativa para o tratamento dessas lesões cutâneas (MURAKAMI *et al.,* 2010; YARISWAMY *et al*., 2013; BARREIROS *et al*., 2014; AGYARE *et al*., 2016).

Entretanto, apesar desse potencial, mais estudos com foco na investigação da atividade cicatrizante e seus possíveis mecanismos de ação, são necessários para subsidiar sua utilização no tratamento de lesões cutâneas.

2 FUNDAMENTAÇÃO TEÓRICA

2.1 Lectinas

A ligação entre as lectinas e seus ligantes ocorre de maneira reversível e pode ocorrer, principalmente, através de pontes de hidrogênio e interações hidrofóbicas (SHARON; LIS, 2004). As lectinas são classificadas, de acordo com sua organização estrutural e os domínios de reconhecimento a carboidrato (DRC), em (PEUMANS; VAN DAMME, 1995; VAN DAMME *et al*., 1998):

Merolectinas: são proteínas que possuem um único domínio ligante a carboidrato; por isso, são incapazes de precipitar glicoconjugados ou aglutinar células.

Hololectinas: são proteínas que possuem dois ou mais domínios de ligação a carboidrato, sendo, então, capazes de precipitar glicoconjugados ou aglutinar células.

Quimerolectinas: são proteínas que possuem um ou mais domínios lectínicos adicionados de outro domínio catalítico em um domínio diferente do ligante a carboidrato.

Superlectinas: são proteínas que possuem dois ou mais domínios ligantes a carboidrato; no entanto, esses domínios possuem especificidade para carboidratos diferentes.

Em geral, a estrutura tridimensional das lectinas é composta por um elevado teor de folhas-β com pouca contribuição das α-hélices, sendo as folhas-β ligadas por alças formando cadeias antiparalelas. A estabilidade de dímeros e tetrâmeros é conferida por interações hidrofóbicas, ligações de hidrogênio e ligações salinas. Os domínios de interação a carboidrato podem ser agrupados em três regiões sobrepostas: a região central, a região em torno do núcleo e a região da zona externa. A região central é constituída por um núcleo conservado, no qual os resíduos interagem com íons metálicos (Mn^{2+} e Ca^{2+}) necessários para as interações com os carboidratos; embora, quase não contribua para a especificidade da lectina ao carboidrato, o núcleo fornece a energia de ligação necessária. Em torno do núcleo, os resíduos aromáticos ocupam posições variáveis em forma de ferradura, sendo essa região a responsável pela especificidade do monossacarídeo à lectina. Finalmente, os resíduos com maior variabilidade estão localizados na zona externa e estão envolvidos em interações com oligossacarídeos ligantes maiores (MACEDO; OLIVEIRA, R; OLIVEIRA, T, 2015).

2.2 Lectinas de plantas

As lectinas são encontradas, nas plantas, em maior concentração, em sementes, podendo constituir em até 10% das proteínas totais das mesmas. No entanto, também são encontradas, mesmo que em baixas concentrações, em outras partes das plantas como frutos, folhas, caules e raízes (SAMPIETRO *et al.,* 2001; LORIS, 2002; SHARON; LIS, 2004; ZANETTI, 2007; PEREIRA *et al.,* 2008; YAN *et al.,* 2010).

As lectinas constituem um grupo bastante complexo e heterogêneo; no entanto, é possível classificá-las com base na relação de estruturas primárias e terciárias presentes em banco de dados com dados de filogenia, formando, assim, sete famílias estruturalmente e evolucionariamente relacionadas (MURDOCK; SHADE, 2002): lectinas de leguminosas, proteínas inativadoras de ribossomos, família das amarantinas, lectinas do floema de cucurbitáceas, lectinas ligantes à manose de monocotiledôneas, lectinas do tipo jacalina e lectinas ligantes à quitina (VAN DAMME *et al.*, 1998).

2.2.1 Lectinas ligantes à quitina

A família das lectinas ligantes à quitina é constituída por todas aquelas lectinas que são capazes de se ligarem a monômeros ou biopolímeros (quitina) de N-acetil-D-glucosamina (GlcNAc), essas podem ou não possuir domínio heveínico. O termo heveína refere-se a uma pequena proteína de 43 resíduos de aminoácidos, encontrado no látex da seringueira (*Hevea brasiliensis*). As lectinas ligantes à quitina são amplamente encontradas nas famílias Gramineae e Solanaceae, mas também são encontradas em espécies como *Triticum aestivum*, *Phytolacca* sp., *Urtica dioica*, *Chelidonium majus* e *Viscum album* (YAO *et al.,* 2010).

2.2.1.1 Aspectos estruturais

O estudo de estruturas tridimensionais de lectinas e de seus complexos com carboidratos ligantes específicos tem aumentado bastante e vários autores têm utilizado esses dados para discutirem as relações evolutivas entre os domínios ligantes à quitina das lectinas. Vários dados mostram que a maioria das lectinas ligantes à quitina de plantas evoluiu a partir de um ancestral comum de heveína, cujos domínios de ligação à quitina são caracterizados por resíduos de aminoácidos

aromáticos e cisteína conservados. Enquanto, os aminoácidos aromáticos estão envolvidos em interações hidrofóbicas com os anéis de glucosamina, permitindo a estabilização do complexo, o alto conteúdo de cisteínas conservadas está envolvido em várias ligações dissulfeto intra-cadeias, dando-lhes rigidez e estabilidade em uma ampla faixa de pH e temperatura (TRINDADE *et al.,* 2006).

Dentre as lectinas ligantes à quitina que já tiveram sua estrutura tridimensional resolvida, pode-se citar a heveína. Essa é uma lectina ligante à quitina isolada do látex da seringueira (*Hevea brasiliensis*) que foi identificada em 1960 (VAN HOLLE; VAN DAMME, 2015; BERTHELOT; PERUCH; LECOMTE, 2016). Sua estrutura tridimensional começou a ser estudada em 1986, apresentando duas α-hélices curtas e uma região de resíduos de aminoácidos localizados na extremidade N-terminal da cadeia polipeptídica que forma duas cadeias antiparalelas de folha-β seguidas por mais uma α-hélice. A estrutura geral da heveína é estabilizada por quatro ligações dissulfeto (BERTHELOT; PERUCH; LECOMTE, 2016).

Uma outra lectina ligante à quitina que também teve sua estrutura tridimensional resolvida foi a UDA, uma lectina monomérica isolada de rizomas da espécie *Urtica dioica.* UDA é uma mistura complexa de várias isolectinas, dentre as quais seis foram isoladas. Em estudos de cristalografia e análises de raios-X, uma dessas isolectinas, denominada UDA-VI, teve sua estrutura tridimensional resolvida, apresentando 89 resíduos de aminoácidos. UDA-VI consistiu de dois domínios, o domínio N-terminal (domínio 1), formados pelos resíduos de 1 a 42, e o domínio C-terminal (domínio 2), formados pelos resíduos de 47 a 89, sendo esses domínios ligados pela sequência Glu43-Arg44-Ser45-Asp46. A estrutura primária da UDA-VI é caracterizada pelo alto teor de resíduos de glicina e cisteína. Ambos os domínios têm quatro ligações dissulfeto e essa é a razão principal para a rigidez e estabilidade de suas estruturas apesar de terem poucas estruturas de folha ou helicoidais. Cada domínio é formado por duas curtas fitas-β, correspondendo aos resíduos Cys17-Ser19 e Cys35-Asn37 (domínio 1) e Cys63-Ser65 e Cys82-Tyr84 (domínio 2), que formam uma estrutura em folha-β antiparalela. O esqueleto principal também é mantido por muitas ligações de hidrogênio entre grupos de peptídeos da cadeia principal (HARATA; MURAKI, 2000; SAUL *et al.,* 2000).

O estudo estrutural dessas lectinas foi muito importante pois, a partir da obtenção de suas estruturas tridimensionais tanto na forma livre quanto complexada com seus ligantes, permitiu uma melhor compreensão do arranjo tridimensional dos

domínios de reconhecimento a carboidrato e a relação desses com suas atividades biológicas, fornecendo informações acerca de seus mecanismos de ação.

2.2.1.2 Aplicação anti-inflamatória

Vários estudos têm descrito as lectinas exógenas como moléculas capazes de interferir em processos inflamatórios. E um dos mecanismos de ação provém da capacidade de inibição do rolamento, adesão e, por consequência, da migração de neutrófilos para o local da infecção. Os neutrófilos desempenham um importante papel no processo de inflamação e, por isso, são as células de defesa mais abundantes na corrente sanguínea do homem. Para que estes possam migrar para os locais da infecção, uma série de moléculas entram em ação, as selectinas (lectinas endógenas). Estas interagem com os carboidratos ou glicoconjugados dos leucócitos, aderindo-os ao endotélio vascular, passo inicial para o extravasamento do endotélio ao local da inflamação. Em um próximo passo, ocorre o processo de adesão ao endotélio vascular através de proteínas chamadas de integrinas (VESTWEBER; BLANKS, 1999; LOWE, 2003; NATHAN, 2006). Dessa forma, as lectinas exógenas inibem a interação neutrófilos-endotélio, competindo ou bloqueando os carboidratos ligantes dos neutrófilos comuns às selectinas.

Visando estudar o papel de resíduos de carboidratos no recrutamento de neutrófilos, foi mostrado que glicoconjugados contendo N-acetil-D-glucosamina são muito importantes nesse processo. A lectina ligante à quitina isolada de *Lonchocarpus sericeus* foi capaz de interagir com esses glicoconjugados presentes nos neutrófilos e, dessa forma, inibindo o rolamento e adesão dos mesmos ao endotélio vascular, em modelo de peritonite e edema de pata. Tal efeito mostrou a dependência do domínio de interação a carboidrato, tendo em vista que a administração simultânea da lectina com seu ligante especifico conseguiu reverter a migração leucocitária (ALENCAR *et al.,*1999).

Uma outra abordagem para se estudar os mecanismos de ação de como as lectinas exógenas estariam inibindo a migração de leucócitos para os locais da infecção seria através da análise de uma via indireta mediada por macrófagos residentes. Sabe-se que os neutrófilos são atraídos quimicamente para o local da infecção e esse processo é mediado por vários fatores quimiotáticos que são liberados pelos macrófagos. Estes, por sua vez, apresentam, em sua superfície celular, ligantes como glicoproteínas e glicolípideos, os quais são reconhecidos como alvos de ligação

das lectinas. Uma vez ativados, os macrófagos liberam vários mediadores inflamatórios que estimulam a migração dos neutrófilos, dentre eles: citocinas e quimiocinas. Dessa forma, as lectinas exógenas inibem a ativação desses macrófagos, competindo ou bloqueando os glicoconjugados ligantes dos macrófagos comuns às lectinas endógenas e, dessa forma, impedindo a migração de neutrófilos (NAPIMOGA *et al.,* 2007; ALENCAR *et al.,* 2003; ALENCAR *et al.,* 2007).

Napimoga e colaboradores (2007) estudaram os mecanismos de ação da Lectina ligante à quitina isolada de *Lonchocarpus sericeus* e perceberam que essa lectina foi capaz de inibir a migração de neutrófilos tanto por interferência em sua adesão ao endotélio quanto pela redução dos níveis de mediadores inflamatórios IL-1β (interleucina 1) e TNF-α (Fator de necrose tumoral), responsáveis pela migração dos neutrófilos, em modelo de peritonite.

2.2.2 Moringa oleifera Lamarck

M. oleifera é também chamada de *M. pterygosperma* Gaertn, pertencente à família Moringaceae, incluindo 12 espécies. É uma planta nativa do Himalaia no norte da Índia, sendo bastante cultivada em países tropicais e subtropicais, recebendo vários outros nomes, tais como “drumstick tree”, “horseradish tree” e “malunggay” (RAMACHANDRAN; PETER; GOPALAKRISHNAN, 1980; MBIKAY, 2012). A planta é bastante utilizada no consumo humano, sendo quase todas as suas partes comestíveis. As folhas, frutos, flores e vagens são bastante utilizadas como alimento em alguns países, particularmente na Índia, Paquistão, Filipinas, Havaí e várias partes da África (ANWAR *et al*., 2007). Uma propriedade bastante conhecida de *M. oleifera* é a de purificação da água, tendo em vista o elevado teor de proteínas catiônicas, nas sementes, com massa molecular entre 6 e 16 KDa e ponto isoelétrico bastante alcalino (FERREIRA *et al*., 2008).

Além das características mencionadas, *M. oleifera* também apresenta uma série de propriedades terapêuticas já relatadas na literatura, dentre as quais podem ser citadas: antibacteriana, antifúngica, anti-inflamatória, hepatoprotetora, anti-hipertensiva, antitumoral, antioxidante, analgésica, hipoglicemiante e hipocolesterolêmica (CHUANG *et al.,* 2007; TALREJA, 2010; FERREIRA *et al.,* 2011; SACHAN; JAIN; SINGH, 2011; MOHAMEDY; ABDALLA, 2014). Além disso, *M. oleifera* também tem sido relatada por apresentar atividade cicatrizante. Estudos com o extrato das folhas, composto de fitoesteróis, glicosídeos, taninos e aminoácidos, e

de sementes mostraram o uso dessa espécie no tratamento de feridas cutâneas (CHOPRA, 1993; RAWAT *et al.,* 2012; BHATNAGAR *et al.,* 2013; SIVARANJANI; PHILOMINATHAN, 2016).

E algumas dessas propriedades estão relacionadas com lectinas que já foram isoladas e relatadas na literatura. Foram isoladas, de sementes de *M. oleifera*, duas lectinas ligantes à quitina, uma lectina solúvel em água (WS*Mo*L) e uma lectina coagulante (c*Mo*L) (SANTOS *et al.,* 2005; SANTOS *et al.,* 2009; PAIVA *et al.,* 2011). A lectina WS*Mo*L apresentou atividade antibacteriana, reduzindo o crescimento das espécies *Staphylococcus aureus* e *Escherichia coli* (FERREIRA *et al.,* 2011). A c*Mo*L atuou como uma proteína anticoagulante em parâmetros de coagulação sanguínea *in vitro* (LUZ *et al.,* 2013). Katre e colaboradores (2008) também isolaram uma lectina de sementes de *M. oleifera* que teve sua atividade hemaglutinante inibida quando incubada com as glicoproteínas fetuína, tiroglobulina e holotransferina.

Nosso grupo de pesquisa também isolou algumas lectinas ligantes à quitina de sementes de *M. oleifera*, estas foram denominadas, de acordo com a ordem em que são eluídas em matriz CM-Sepharose, *Mo*-CBP$_2$, *Mo*-CBP$_3$ e *Mo*-CBP$_4$ (*Mo*: *M. oleifera*, CBP: “Chitin Binding Protein”). *Mo*-CBP$_2$ foi capaz de inibir o crescimento de *Candida albicans*, aumentando a permeabilidade da membrana e induzindo a produção de espécies reativas de oxigênio endógenas (SILVA NETO, 2015). *Mo*-CBP$_3$ apresentou atividade inibitória contra os fungos fitopatogênicos *Fusarium solani, Fusarium oxysporum, Colletotrichum musae* e *Colletotrichum gloesporioides*, a mesma foi capaz de aumentar a permeabilidade da membrana celular, interferindo nas bombas de H+-ATPase e induzindo estresse oxidativo (GIFONI *et al*., 2012; BATISTA *et al*., 2014). *Mo*-CBP$_4$ mostrou atividade contra o fungo dermatófito *Trichophyton mentagrophytes* e apresentou atividades antinociceptiva e anti-inflamatória, quando administrada em camundongos via oral (PEREIRA *et al*., 2011; PEREIRA, 2014; LOPES, 2016).

No entanto, a única lectina isolada de *M. oleifera* a ter sua estrutura tridimensional resolvida foi a *Mo*-CBP$_3$. Esta é formada por quatro isoformas, denominadas *Mo*-CBP$_3$-1, *Mo*-CBP$_3$-2, *Mo*-CBP$_3$-3 e *Mo*-CBP$_3$-4, que diferem entre si por uns poucos resíduos de aminoácidos. *Mo*-CBP$_3$-1, consistindo de 163 aminoácidos, teve a estrutura de seu cristal determinada em uma resolução de 1,7 Å e mostrou ser formada por α-hélices e loops. Apresentou-se como uma unidade assimétrica, consistindo em duas cadeias polipeptídicas, uma cadeia leve (resíduos

37 a 63) e uma cadeia pesada (resíduos 93 a 158). A estrutura em α-hélice consistiu de cinco hélices conectadas por curtos loops. As cadeias são estabilizadas por duas pontes dissulfeto (Cys41-Cys110 e Cys54-Cys99) e duas pontes dissulfeto intra-cadeias (Cys100-Cys148 e Cys112-Cys155) dão uma estabilidade adicional à cadeia pesada (ULLAH *et al.,* 2015).

2.2.3 Mo-CBP$_4$ (*Moringa oleifera-Chitin Binding Protein*)

Mo-CBP$_4$ trata-se de uma proteína básica, apresentando ponto isoelétrico de 10,55, formada por duas cadeias de massas moleculares distintas, uma menor com 3,88 KDa e uma maior com 8,43 KDa, ligadas por pontes dissulfeto, apresentando uma massa molecular total de 11,78 KDa. Apresentou também propriedades floculantes que parecem estar associadas ao seu caráter catiônico, principalmente, devido à presença de um grande número de resíduos de aminoácidos do tipo arginina e histidina em sua composição, os quais contribuem para interações eletrostáticas com cargas negativas de certas partículas como por exemplo, de argila e bactérias, reduzindo a repulsão eletrostática e levando a aglomeração de partículas (PEREIRA, 2014).

Foi mostrado que *Mo*-CBP$_4$, em condições nativas (pH 7,0 e 25 °C), é composta por 35% de α-hélices, 15% de folhas-β, 19% de voltas e 30% de estruturas desordenadas. Estas estruturas se mantiveram mesmo quando a proteína foi submetida a variações de pH e temperatura, mostrando sua elevada estabilidade. Resistência também foi encontrada quando *Mo*-CBP$_4$ foi submetida à degradação proteolítica com pepsina, tripsina e quimiotripsina, separadamente ou em conjunto. Ademais, testes de estabilidade mostraram que *Mo*-CBP$_4$ pode ser armazenada por um período longo (6 meses), à temperatura ambiente, sem perder sua elevada solubilidade em água, sua capacidade de se ligar à quitina e suas atividades anti-inflamatória e analgésica (COELHO, 2013; PEREIRA, 2014).

Em relação às atividades biológicas, *Mo*-CBP$_4$ foi capaz de inibir em 50% a germinação de conídios de *T. mentagrophytes* em uma concentração mínima de 500 µg/mL. Tal atividade pareceu estar associada a um aumento da permeabilidade da membrana dos conídios e indução da produção de espécies reativas de oxigênio endógenas (LOPES, 2016). Além disso, *Mo*-CBP$_4$, em um modelo experimental de contorção abdominal, induzido por ácido acético, *Mo*-CBP$_4$, na dose de 10 mg/Kg, foi capaz de inibir em 98,9% (por via intraperitoneal) e 52,9% (por via oral) o número de

contorções abdominais em camundongos (PEREIRA *et al.,* 2011). Posteriormente, em um modelo de peritonite em ratos, induzida por carragenina, *Mo*-CBP$_4$, na dose de 0,1 mg/Kg (por via endovenosa), foi capaz de inibir em 79% a migração de neutrófilos para o local da inflamação. Entretanto, os resultados mais promissores foram encontrados quando a proteína foi administrada por via oral. Em um modelo de peritonite em camundongos, induzida por zymosan, *Mo*-CBP$_4$, na dose de 40 mg/Kg, foi capaz de reduzir em 48% a migração de neutrófilos e ainda reduzir os níveis da citocina pró-inflamatória IL-1β e aumentar os níveis da citocina anti-inflamatória IL-10 no soro dos animais. A atividade anti-inflamatória de *Mo*-CBP$_4$ foi inibida quando a mesma foi pré-incubada com seu ligante específico, o GlycNac, revertendo completamente a migração de neutrófilos, sugerindo a participação do domínio de interação a carboidrato nessa atividade (PEREIRA, 2014).

2.3 Cicatrização

As feridas são lesões físicas, químicas ou térmicas que resultam numa abertura ou quebra na integridade da pele ou podem também ser definidas como a interrupção da integridade anatômica e funcional do tecido vivo. De acordo com a *Wound Healing Society*, as feridas são lesões físicas que resultam em uma abertura ou ruptura da pele, causando distúrbio na anatomia e função da pele normal. Resultando ainda na perda de continuidade do epitélio com ou sem a perda de tecido conjuntivo subjacente (RAMZI; VINAY; STANLEY, 1994; STRODTBECK, 2001). Estimativas atuais indicam que quase 6 milhões de pessoas sofrem de feridas crônicas em todo o mundo (PERCIVAL, 2002; MATHIEU; LINKE; WATTEL, 2006; KRISHNAN, 2006; AGYARE *et al*., 2016).

O processo de cicatrização é uma série complexa de eventos inter-relacionados que são mediados em suas diferentes fases por uma ampla gama de processos celulares quimicamente coordenados, bem como influências hormonais. Além disso, é caracterizado por uma série de eventos independentes e sobrepostos. O processo pode ser categorizado em quatro etapas: fase da hemostasia (coagulação), fase inflamatória, fase proliferativa (formação de tecido de granulação e síntese de colágeno) e finalmente a fase de remodelação que, em última instância, determina a força e aparência do tecido curado (AGYARE *et al*., 2016). O processo cicatricial é induzido pela produção de citocinas pró-inflamatórias no tecido lesionado, pois favorecem a fase inflamatória a fim de reparar o tecido. No entanto, quando

produzidas em altas concentrações dificultam a evolução do processo devido à instabilidade hemodinâmica ou distúrbios metabólicos. Por isso, citocinas anti-inflamatórias são liberadas, no local da lesão, no intuito de modular a inflamação, regulando, assim, a migração de neutrófilos e monócitos para o local da lesão e inibindo a produção de citocinas pró-inflamatórias (OLIVEIRA *et al.,* 2011; SÜNTAR *et al.* 2011).

Esse processo de cicatrização cutânea é de grande interesse para a saúde pública, uma vez que a existência de feridas na pele reduz a qualidade de vida do paciente e levam a um prolongado tempo de tratamento e, com isso, à gastos exorbitantes. Com isso, várias formas de tratamento têm sido desenvolvidas para o controle de lesões cutâneas, incluindo pomadas, hidrogéis e curativos. (MURAKAMI *et al.*, 2010; BARREIROS *et al*., 2014). No entanto, as características de um curativo ideal, tais como a eficácia na absorção de exsudados de feridas, flexibilidade, durabilidade, aderência e baixo custo, ainda não foram totalmente atingidas (PEREIRA *et al.,* 2016). Um tratamento ideal desses tipos de feridas compreende ainda características como prevenção de infecções, manutenção de um ambiente úmido para a ferida, permeabilidade ao vapor de água, baixa aderência para reduzir a dor durante a remoção e baixa frequência de mudança (ALBERTINI *et al.,* 2013). Portanto, a descoberta de novos tratamentos é de grande importância.

Atualmente, o foco dos estudos, no tratamento de feridas, é o desenvolvimento de curativos mais eficientes e menos dispendiosos, que sejam biocompatíveis e biodegradáveis para fornecer melhores condições para a cicatrização de feridas e melhorar a qualidade de vida dos pacientes (MOURA *et al*., 2013).

3 HIPÓTESE

“*Mo*-CBP$_4$, uma proteína ligante à quitina presente em sementes de *Moringa oleifera*, é capaz de modular a resposta inflamatória da cicatrização, acelerando a reparação tecidual de lesões na pele, sendo a determinação de sua estrutura tridimensional essencial para o entendimento dessa atividade biológica. Apresentando-se, portanto, como potencial ferramenta biotecnológica no tratamento tópico de feridas cutâneas.”

4 OBJETIVOS

4.1 Geral

Determinar a estrutura tridimensional de *Mo*-CBP$_4$, uma proteína ligante à quitina de sementes de *Moringa oleifera* com atividade anti-inflamatória, e avaliar seu efeito sobre o processo cicatricial de feridas cutâneas excisionais.

4.2 Específicos

- Purificar *Mo*-CBP$_4$ a partir de sementes de *Moringa oleifera*;
- Obter a sequência primária completa de *Mo*-CBP$_4$;
- Obter e difratar os cristais de *Mo*-CBP$_4$;
- Resolver e analisar a estrutura cristalográfica de *Mo*-CBP$_4$;
- Propor um veículo para a aplicação tópica de *Mo*-CBP$_4$ sobre feridas cutâneas excisionais em camundongos;
- Analisar macro- e microscopicamente o efeito de *Mo*-CBP$_4$ sobre feridas cutâneas excisionais em camundongos;
- Determinar os mecanismos de ação de *Mo*-CBP$_4$ envolvidos no processo cicatricial de feridas cutâneas excisionais;
- Avaliar a atividade tóxica de *Mo*-CBP$_4$ em cultura celular.

5 ARTIGO 1 REFERENTE À TESE

Título

Structural characterization of a lectin from *Moringa oleifera* seeds with anti-inflammatory activity

Autoria

Tiago D.P. Lopes[1]*, Lucas P. Dias[2], Larissa A.L. Souza[1], Mirella L. Pereira[3], Eduardo H.S. Bezerra[1], Helen P.S. Costa[4], João X.S. Neto[4], Fábio C.S. Nogueira[5], Bruno A.M. Rocha[1], Nylane M.N. Alencar[6], José T.A. Oliveira[1], Ilka M. Vasconcelos[1], Daniele O.B. Sousa[1]*

[1]Department of Biochemistry and Molecular Biology, Federal University of Ceará, Fortaleza, Ceará, Brazil.

[2]Department of Biophysics, Paulista School of Medicine, Federal University of São Paulo, São Paulo, SP, Brazil.

[3]Department of Biology, Federal University of Ceará, Fortaleza, Ceará, Brazil.

[4]Biotechnology and Molecular Biology Laboratory, State University of Ceará, Fortaleza, Ceará, Brazil.

[5]Institute of Chemistry, Federal University of Rio de Janeiro, Rio de Janeiro, Brazil.

[6]Department of Physiology and Pharmacology, Federal University of Ceará, Fortaleza, Ceará, Brazil

*Corresponding authors. E-mail address: t.deiveson@gmail.com (LOPES, T. D. P.) and daniele.sousa@ufc.br (SOUSA, D.O.B.).

ABSTRACT

Lectins are proteins of nonimmune origin widely found in plants, animals and microorganisms. These proteins can binding reversibly to specific carbohydrates and are involved in several biological events. In this work, we establish the primary and three-dimensional structure the *Mo*-CBP$_4$, a lectin purified from *Moringa oleifera* seeds, and we assessment its anti-inflammatory effect. *Mo*-CBP$_4$ (11,780 KDa) is composed of 99 amino acid residues distributed in two subunits: light chain (3,888 KDa) and heavy chain (8,428 KDa). Crystallization datas demonstrate that *Mo*-CBP$_4$ has a typical alpha-helical structure, with five helices distributed between the two chains. In addition, there are two inter-chain Cys-Cys bridges and two intra-chain bridges. *Mo*-CBP$_4$ presented anti-inflammatory activity, decreasing neutrophil migration and modulating pro and anti-inflammatory cytokines in a model of peritonitis. Furthermore, *Mo*-CBP$_4$ was able to attenuate the mechanical hypernociception induced by carrageenan. Molecular docking results demonstrate that *Mo*-CBP$_4$ has high affinity for N-Acetylglucosamine (GlcNAc) indeed, the lectin had its anti-inflammatory activity reversed when pre-incubated with GlcNAc. These results indicate that the biological activities of *Mo*-CBP$_4$ can be related with the interaction between the lectin domain and glycans in specific molecular targets. *Mo*-CBP$_4$ can be applied as a tool in studies of inflammation and hypernociception.

Keywords: *Moringa oleifera*, lectin, structural characterization, anti-inflammatory, anti-hypernociceptive.

5.1 Introduction

Lectins are defined as proteins or glycoproteins of nonimmune origin and which are capable of recognizing and reversibly binding specific mono- or oligosaccharides without altering their chemical structures. These molecules were initially found and described in plants, but also were isolated from microorganisms and animals (VAN DAMME et al., 1998; GHAZARIAN; IDONI; OPPENHEIMER, 2011). Although more widely studied, the role of plant lectins is still not well understood (TSANEVA; VAN DAMME, 2020). This group of lectins has gained great importance in the biotechnology field and much of this importance depends on the interaction of the lectin with some glycosidic component. The plant lectins have already been reported exerting the most varied activities, such as insecticide (CHETTRI et al., 2021), antifungal (CAVADA et al., 2021; MISHRA et al., 2019), bactericidal (SANTOS et al., 2021), antitumor (BHUTIA et al., 2019) and anti-inflammatory (HIREMATH et al., 2020; CARNEIRO et al., 2021; WANG et al., 2020).

Chitin-binding lectins is a group consisting of all those lectins which are capable of binding to monomers or biopolymers (chitin) of N-acetyl-D-glucosamine (GlcNAc) (YAO et al., 2010). Experimental models of inflammation have demonstrated that chitin-binding lectins are able to modulate the inflammatory process by inhibiting neutrophil migration through interaction with glycoconjugates containing N-acetyl-D-glucosamine present in neutrophils (ALENCAR et al., 2019; NAPIMOGA et al., 2007).

Moringa oleifera LAM. is also called *M. pterygosperma* Gaertn, belonging to the family Moringaceae which includes 12 species. It is a plant native to the Himalayas in northern India, and is widely cultivated in tropical and subtropical countries, receiving several other names such as "drumstick tree", "horseradish tree" and "malunggay" (PADAYACHEE; BAIJNATH, 2020; POPOOLA et al., 2020). This plant presents significant socio-economic value as it is used for food and herbal medicine (NOVA et al., 2020; GEORGE et al., 2021).

In previous study, a chitin-binding lectin (*Mo*-CBP$_4$) was purified from *M. oleifera* seeds and showed an apparent molecular mass of 9.8 KDa under reducing conditions. In addition, it presented flocculant activity, which is a characteristic of the aqueous extracts obtained from its seeds. In contrast to the other lectins found in *M. oleifera* seeds, *Mo*-CBP$_4$ was not able to agglutinate rabbit or human erythrocytes, despite being a protein that binds to the monomers or biopolymers of GlcNAc. In an

experimental model of pain induced by acetic acid, *Mo*-CBP$_4$ inhibited the number of abdominal contortions at a dose of 10 mg/kg in 98.9% and 52.9% when administered intraperitoneally and orally, respectively. The lectin also showed considerable anti-inflammatory activity since it was able to inhibit the increase of vascular permeability in 89.1% also in the dose of 10 mg/kg, using acetic acid as a phlogistic agent (PEREIRA et al., 2011). Furthermore, *Mo*-CPB$_4$ also showed a potent antidermatophytic activity. The protein reduced in 50% the germination of microconidia of *Trichophyton mentagrophytes* (at concentration of 45 µM). The *Mo*-CBP$_4$ treatment caused an increase in membrane permeability, damage to cell wall and ROS overproduction, leading to microconidia death. *Mo*-CBP$_4$ (5, 10 and 20 mg g^{-1}) also reduced the severity and time of dermatophytosis *in vivo* models (LOPES et al., 2020).

Therefore, this study aimed to establish the primary and three-dimensional structure of *Mo*-CBP$_4$. The anti-inflammatory effect was performed, and structure-activity relationship was analyzed by molecular docking.

5.2 Materials and methods

5.2.1 Plant material

M. oleifera seeds were collected from trees at Pici Campus of Federal University of Ceará (UFC), Fortaleza, Brazil. A voucher specimen (Nº EAC34591) was deposited in the Prisco Bezerra Herbarium, UFC.

5.2.2 Protein extraction and purification

Purification of *Mo*-CBP$_4$ was performed following protocol described by Pereira *et al*. (2011) with modifications. Mature seeds were ground in a coffee grinder and treated with n-hexane (1:10, w/v). Defatted flour was extracted with 50 mM Tris-HCl buffer, pH 8.0, containing 150 mM NaCl (1:10 w/v), for 4 h at 4 °C, filtered through cheesecloth and centrifugated at 15,000 x *g*, 4 °C, 30 min. Next, the supernatant was exhaustively dialyzed against distilled water and centrifuged again under the same conditions. The soluble proteins (albumin fraction) resuspended in extraction buffer was submitted to affinity chromatography (chitin matrix) previously equilibrated with the above buffer. The *M. oleifera* chitin-binding proteins (*Mo*-CBPs) were eluted with 50 mM acetic acid, pooled and dialyzed against distilled water at 4° C. *Mo*-CBPs fraction in 50 mM sodium acetate buffer, pH 5.2 was applied to a cation-exchange matrix (CM-Sepharose^{TM}) pre-equilibrated with the same buffer. The Adsorbed proteins were eluted by stepwise method with increasing NaCl concentrations. *Mo*-CBP$_4$ (*Mo*: *M. oleifera*; CBP: Chitin-Binding Protein) corresponds as the peak eluted with 600 mM NaCl.

5.2.3 Sequencing and analysis of the primary structure

5.2.3.1 Mass spectrometry

Mo-CBP$_4$ (1 mg) was resuspended in 10 µL of 10 mM ammonium bicarbonate. The protein dosage was done by fluorometry using Qubit® 2.0 Fluorometer (Thermo Fisher). For proteolytic cleavage, 40 µg of the protein was used for each digestion assay, varying the enzyme used. Trypsin (Promega) and chymotrypsin (Sigma-Aldrich) were used at 1:50 w/w and 1:75 (enzyme/substrate) respectively. Trypsin cleavage was performed at the 18- and 5-hours periods at 35 °C. For chymotrypsin cleavage, the period was 12 hours at room temperature (25 °C). After digestion, the samples were desalted in Poros-20 R2 reverse phase resin and

C18 filter, with the peptides eluted in 50% and 70% acetonitrile and 0.1% TFA. Afterwards, they were concentrated under vacuum (RVC 2-25 CDplus - CHRIST), resuspended in 0.1% formic acid and dosed by fluorometry. Peptides obtained in different proteolytic cleavages were analyzed by mass spectrometry coupled to reverse phase liquid chromatography in nano-flow (nLC-MS/MS-EASY) performed in ESI LTQ Orbitrap Velos (Thermo Scientific) in DDA (Data Dependent Analysis) mode. For the chromatography, a pre-column (2 cm long x 200 µm ID) packed with ReproSil-Pur C18-AQ 5 µm resin and a New Objective PicoFrit® analytical column (25 cm long x 100 µm ID) packed with ReproSil-Pur C18-AQ 3 µm resin were used. The spectra obtained were analyzed in the Proteome Discoverer™ 2.1 program (Thermo Fisher), considering only the high reliability results were selected. *Mo*-CBP$_4$ primary sequence was subjected to analysis by bioinformatics to determine homology/similarity with other proteins in the database of the National Center of Biotechnology Information (NCBI), using BLASTp. The most similar proteins were selected for alignment using ESPript 3.0.

5.2.3.2 N-terminal sequence analysis

To determine the N-terminal sequence of *Mo*-CBP$_4$, the isolation of its subunits was initially done. The reduced and alkylated protein (10 mg/mL) was desalted using a Sephadex® G-25 (GE Healthcare) column. The sample was then subjected to C18 column reverse phase chromatography (4.6 x 100 mm) coupled to the HPLC system (Waters) using a linear gradient (5-90%) of acetonitrile (ACN) for 50 minutes, at a flow rate of 0.2 mL/minute. For this purpose, solvent A (5% ACN, 95% H_2O containing 0.05% TFA) and solvent B (90% ACN) were used. Chromatography was monitored for absorbance at the wavelength of 230 nm. To obtain the N-terminal amino acid sequence of the *Mo*-CBP$_4$ chains, an automatic protein sequencer (Shimadzu PPSQ-23A), based on the Edman degradation principle, was used. Phenylthiohydantoin derivatives of amino acids (PTH-amino acids) were detected at 269 nm after C18 reverse phase (4.6 x 2.5 mm) column separation, conducted under isocratic conditions according to the manufacturer's instructions. The amino acid sequence obtained was subjected to comparative analysis through the NCBI-BLAST system. The proteins that demonstrated the best percentage of identity were selected and aligned with the aid of the Clustal Omega program (http://www.ebi.ac.uk/Tools/msa/clustalo/) and analyzed.

5.2.4 Determination of the molecular mass

The analysis was performed using an ESI-TOF type in Synapt HDMS mass spectrometer (Waters, Manchester, UK) coupled to a NanoACQUITY UPLC system. *Mo*-CBP$_4$ was analyzed both in its whole and reduced form. For reduction, 50 µL of a 1 mg/mL solution of the protein in 1% formic acid was heated for 15 minutes at 80 °C. Thereafter, 2.5 µL of 0.1 M dithiothreitol was added and heated at 60 °C for 20 minutes for complete reduction of the chains. Alkylation of the exposed sulfhydryl groups was performed by adding 2.5 µL of 0.3 M iodoacetamide, protecting from light. Ten microliters of the sample (reduced or not) were first subjected to reverse phase chromatography on a C18 BEH (1.7 mm × 100 mm × 10 cm) column coupled to UPLC using a gradient of 5 to 80% (v/v) of acetonitrile in 0.1% (v / v) formic acid in a continuous flow of 600 nL/minute. *Mo*-CBP$_4$ spectra were processed using a maximal entropy technique (MaxEnt).

5.2.5 Crystallization

The appropriate concentration of *Mo*-CBP$_4$ (50 mg/mL) to obtain the crystals was defined using the Pre-Crystallization Test (Hampton Research). Hanging-drop crystallization experiments were conducted with *Mo*-CBP$_4$ in 0.02 M sodium acetate at pH 4.6 with 0.1 M NaCl using Crystal Screen I and II kits (Hampton Research, São Paulo, Brazil) to determine the best conditions. Crystals were screened at room temperature (293 K) in vapor-diffusion 24-well Linbro cell-culture plates. The drops were composed by protein solution (1 µL) mixed with an equal volume of crystallization solution and then, this mixture was equilibrated against 300 µL of the crystallization solution placed in the plate.

5.2.6 Data collection

The X-ray diffraction data were collected at a wavelength of 1.42 Å using a synchrotron-radiation source on a MX2 Station of the National Laboratory of Synchrotron Light (LNLS - Campinas, Brazil) at 100K with a PILATUS 2M^{TM} detector (Dectris, Switzerland) placed 150 mm from the crystal. To avoid ice formation, a cryoprotectant (20% glycerol) was added to crystallization reagent. The crystals were rotated through 360° with a 0.2° oscillation range per frame using a fine ϕ-slicing strategy, collecting a total of 1800 frames.

5.2.7 Data processing and structural determination

X-ray diffraction data collected were processed with XDS (KABSCH, 2010) and scaled using SCALA in the CCP4 Program (COLLABORATIVE COMPUTATIONAL PROJECT, 1994). Crystal belongs to the space group $P4_122$ and the calculated Matthews coefficient (2.69 Å3 Da^{-1}) indicated the presence of one molecule in the asymmetric unit (MATTHEWS, 1968). The crystal structure was determined by molecular replacement using PHASER program (MCCOY, 2007). The atomic coordinate used as a model was obtained from deposited *Mo*-CBP_3 structure (PDB code: 5DOM) (ULLAH et al., 2015). The initial generated structure was submitted to restrained refinement using PHENIX (ADAMS et al., 2010; AFONINE et al., 2012; ECHOLS et al., 2012) and then modeled using COOT program (EMSLEY et al., 2010). After addition of 57 water molecules and two chloride ions, a second restrained refinement was performed resulting in a R*factor* of 19.8% and a R*free* of 22.7%. The stereochemistry of the structure was assessed using a Ramachandran plot analysis with MOLPROBITY program (CHEN et al., 2010). All structural figures were generated using PyMOL (DELANO; LAM, 2005).

5.2.8 Molecular docking

Mo-CBP_4 interaction with N-acetyl-D-glucosamine (GlcNAc) was investigated *in silico* using AUTODOCK. Firstly, blind dockings were configured to search, in the entire surface of the crystallized protein, suitable pockets for the interaction with GlcNAc. *Mo*-CBP_4 was prepared for docking using AUTODOCKTOOLS 1.5.6 (MORRIS et al., 2009), adding polar hydrogens and partial charges using the Kollman united-atom and Gasteiger charges, respectively, and size up the docking grid, as well add flexible torsions to GlcNAc assigned to rotate freely.

5.2.9 Indirect Hemagglutinating activity

Mo-CBP_4 samples of 1 mg/mL were incubated with anti-*Mo*-CBP_4 antibodies (1:1, v/v) previously produced in rabbits. The hemagglutinating activity assay was performed in microtiter plates (MOREIRA; PERRONE, 1977). The samples were serially diluted, and the capacity to agglutinate 3% rabbit erythrocytes was evaluated in suspension (native and treated with the proteolytic enzyme trypsin). The sugar specificity of *Mo*-CBP_4 was tested by comparing the ability of carbohydrates to inhibit erythrocyte agglutination caused by lectin previously bound to the antibody. For

the inhibition assays, serial dilutions (initial concentration: 100 mM) of N-acetyl-D-glucosamine, D-glucose and D-mannose were performed before addition of *Mo*-CBP$_4$.

5.2.10 Biological activities

5.2.10.1 Animals

Female Swiss mice, weighing 20-30 g, were provided by the Animal House of UFC. The animals were housed in groups of five in polypropylene cages at room temperature (25 ± 3 °C) and exposed to a 12 h dark/12 h light cycle. Both food and water were offered *ad libitum*. Twelve hours before experimentation, they were transferred to the laboratory and housed only with water *ad libitum*. The experimental protocols were performed in accordance with the current guidelines for the care of laboratory animals and the ethical guidelines for investigations of experimental pain in conscious animals, reviewed and approved by the Animal Ethics Committee of UFC, Brazil (protocol number: 86/10).

5.2.10.2 Zymosan A-induced peritonitis

The procedure used to zymosan A-induced peritonitis was the same as described previously by Doherty *et al.* (1985) and Kolaczkowska, Seljelid and Plytycz (2001). Mice were treated with *Mo*-CBP$_4$ (10, 20 and 40 mg/kg, p.o.) and after 1 hour, the inflammatory stimulus was generated by injection of zymosan A (Sigma-Aldrich) freshly prepared in 0.9% saline (2 mg/cav.). Dexamethasone (5 mg/kg, i.p.) or saline were used as positive and normal controls, respectively. Four hours later, the animals were euthanized, and peritoneal cavities were washed with 3 mL sterile saline containing 5 IU/mL heparin. Total and differential cells were counted, and the results were expressed as mean ± SEM of the number of cells per microliter of peritoneal fluid. In order to investigate the structural requirements of the *Mo*-CBP$_4$ to display inhibitory activity on neutrophil migration, the protein was incubated with 0.1 M N-acetyl-D-glucosamine (GlcNAc) at 37 °C for 1 h and submitted to heat treatment at 100 °C for 1 h before using in the experiments as described.

5.2.10.3 Cytokines measurement

Levels of cytokines (IL-1β, TNF-α and IL-10) were measured from the serum of animals treated with *Mo*-CBP$_4$ (40 mg/kg; p.o.) or saline previously zymosan A-induced peritonitis. To obtain serum, after 3 hours of the inflammatory stimulus, the

animals were euthanized, and blood was collected from retro-orbital plexus and centrifuged at 600 x g for 10 min. To quantify TNF-α, IL-1β and IL-10 was used ELISA method (CUNHA et al., 2000). Microtiter plates (96 wells) were coated with 50 µl PBS buffer containing 2.0 µg/mL of monoclonal anti-IL-1β, anti-TNF-α or anti-IL-10 from sheep serum. The plates were incubated for 12 hours at 4 °C and washed 3 to 5 times with PBS containing 0.05% Tween 20. Thereafter were added 50 µL of 1% bovine serum albumin (blockade solution) and incubation proceeded for 2 hours at room temperature. The plates were again washed as described above and then added to the test samples in triplicate. Standard curves were obtained using increasing concentrations of IL-1β, TNF-α and IL-10 diluted in PBS-Tween. After 24 hours incubation at 4 °C, was added biotinylated monoclonal anti-IL-1β, anti-TNF-α and anti-IL-10 diluted 1% BSA and 0.05% Tween. After 1 hour at room temperature, the plates were washed and added to 50 µL of HRP-avidin complex diluted 1:5000. The reaction was stopped with 1 M H_2SO_4 and the absorbance was measured spectrophotometer at 490 nm. The concentration of cytokines was determined from the standard curve. The results were expressed as picograms of cytokines/mL of serum.

5.2.10.4 Mechanical hypernociception

For the evaluation of mechanical hypernociception was used a calibrated electronic von Frey anesthesiometer (Electronic von Frey; IITC Life Science, Woodland Hills, CA) described by Cunha *et al.* (2007). Briefly, in a quiet room, mice were placed individually in acrylic cages (12 × 20 × 17 cm) with grid floors, 15-30 min before the test, for allow environmental adaptation. The test consists on applying a gradually increasing pressure in the plantar surface of the hind paw using a transducer adapted with a 0.5 mm^2 polypropylene tip which evoking a paw flexion reflex. The end point was indicated by withdrawal of the paw and the pressure intensity was recorded. The animals were tested before (basal reaction) and after treatments. The value for the response was an averaging of three measurements and the results are expressed by Δ withdrawal threshold (in grams, g), which was calculated by subtracting the measurements before treatment minus after treatment. *Mo*-CBP_4 (40 mg/kg) was administered orally, and after 1-hour, carrageenan (Cg) was injected into hind paws (300 mg/paw) to cause inflammatory hypernociception. The animals were then submitted to von Frey test at 1, 3, and 5 h after the inflammatory stimulus (Cg).

Indomethacin (5 mg/kg, i.p.) or saline were used as positive and normal controls, respectively.

5.2.10.5 Myeloperoxidase (MPO) assay

The MPO activity indicates indirectly the neutrophil infiltration into tissues, based on a kinetic-colorimetric assay as described previously (BRADLEY et al., 1982). To investigate potential effect on neutrophil accumulation into plantar tissues, mice were treated with *Mo*-CBP$_4$ (40 mg/kg, p.o.) and after 1 h, carrageenan (300 mg/paw) was injected into the hind paw. After 3 h, the animals were euthanized, and their paws were removed. Samples of plantar tissue were triturated and homogenized in 50 mM phosphate buffer (pH 6.0) added of 0.5% hexadecyl trimethylammonium bromide (HTAB). After centrifugation at 1,500 x *g* for 15 min, at 4 °C, the supernatant was used to assay. At 96-well microplate, 10 µL of supernatant were added to 200 µL of 50 mM phosphate buffer (pH 6.0), containing 0.167 mg/mL O-dianisidine dihydrochloride and 0.0005% hydrogen peroxide. MPO activity was measured taking three readings in 1 min at 450 nm at microplate reader. A standard curve was realized using neutrophils of mouse blood to compare of MPO activity. The results were presented as number of neutrophils × 10^6/mg.

5.2.10.6 Statistical analysis

All results were expressed as mean ± S.E.M. for groups of 5 animals. Statistical evaluation was performed by analysis of variance (ANOVA) followed by Bonferroni's test. A p value of 0.05 was considered significant.

5.3 Results

5.3.1 Primary structure

For elucidation of *Mo*-CBP$_4$ amino acid sequence, the protein was digested with trypsin and chymotrypsin. The complete primary structure was obtained from the overlapping regions of the 40 mass spectrometry peptides and N-terminus sequences (Fig. 1). The polypeptide chain of *Mo*-CBP$_4$ includes 99 amino acid residues distributed in two subunits: the light chain comprising residues 1–30, and the heavy chain comprising residues 31–99. Since nine residues could not be determined by MS/MS, they were established by electron density data and compared with homologous proteins (Fig. 2).

The molecular mass determined by ESI–TOF for the full-length chain (11,780 KDa), light chain (3,888 KDa) and heavy chain (8,428 KDa) agrees with the theoretical mass obtained from the determined sequence: 11,516 KDa; 3,603 KDa and 7,931 KDa for full-length, light and heavy chain, respectively. This result reveals the reliability of *Mo*-CBP$_4$ obtained sequence.

5.3.2 Crystallization and overall structure

The best crystals were obtained using 0.1 M sodium acetate at pH 4.6 with 2.4 M NaCl. Bipyramidal crystals grew after 20 days at room temperature (293 K) (Fig. 3). A complete data set was collected at a resolution of 1.57 Å and scaled to 1.9 Å for suitable crystallographic statistics. The 2S albumin *Mo*-CBP$_3$, the closest homologue of *Mo*-CBP$_4$, shares 73% identity, using the structure 5DOM as a searching model. The final model structure of *Mo*-CBP$_4$ was refined to 1.9 Å. The crystallographic and refinement data are presented in Table 1. The asymmetric unit of the [*Mo*-CBP$_4$-1 PDB code 6VJ0] crystal structure contains one *Mo*-CBP$_4$ monomer. The structure is composed by two covalent-linked polypeptide subunits, the light and heavy chains, comprising the residues 4-28 and 4-68, respectively. These two chains are crosslinked by two inter-chain Cys-Cys bridges (A5-B20 and A18-B9 disulfide bond) and two intra-chain bridges (B18-B9 and B22-B65 disulfide bond). *Mo*-CBP$_4$ is a typical alpha-helical structure, presenting five helices distributed between light (h1-h2) and heavy (h3-h5) chains (Fig. 4a, b).

Figure 1 - Primary structure of *Mo*-CBP$_4$ obtained by overlapping peptides generated by cleavage with trypsin and chymotrypsin.

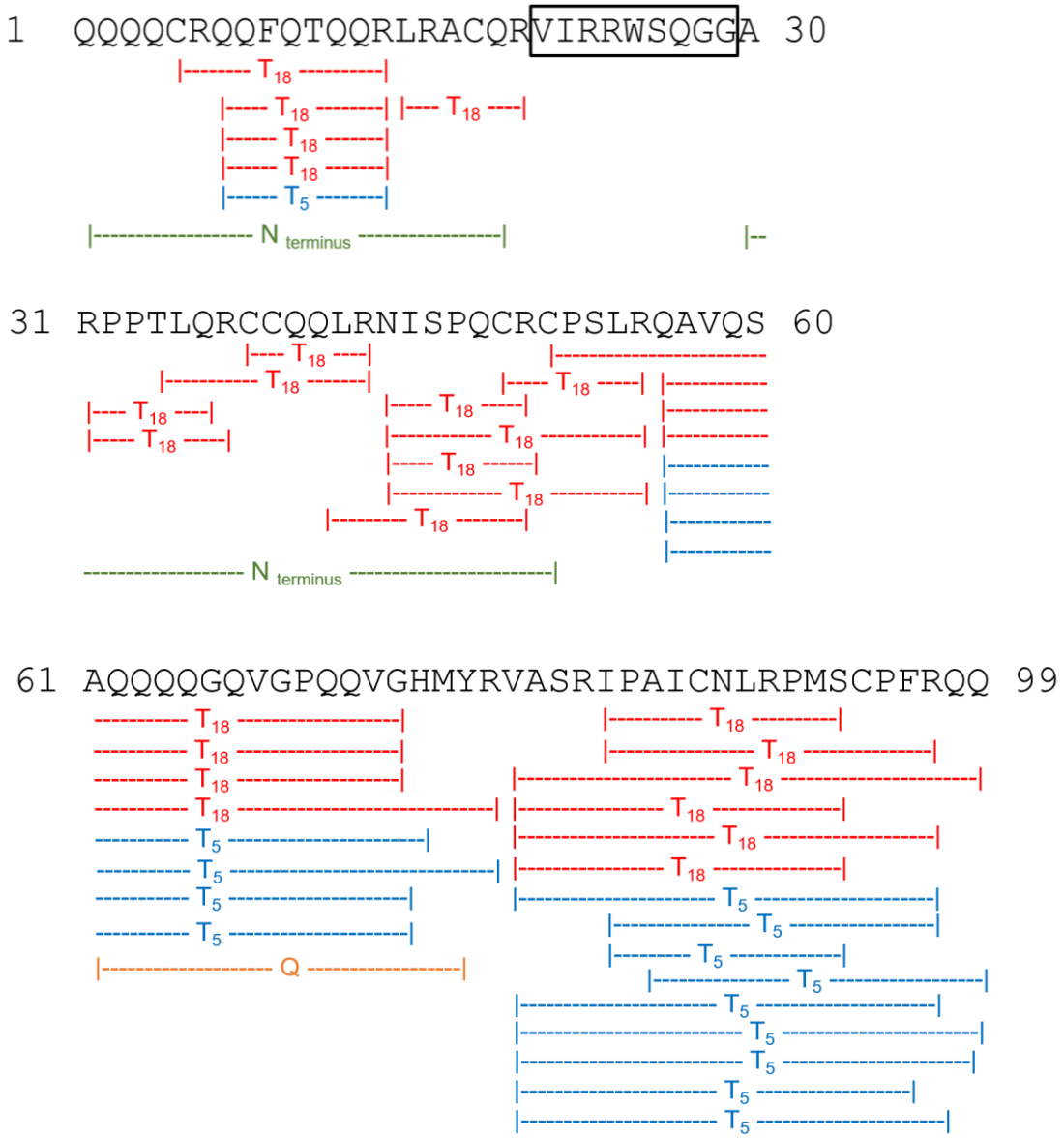

Source: prepared by the author.
The box indicates residues identified by electron density map fit and homology.

Figure 2 - Multiple alignment of proteins similar to *Mo*-CBP$_4$: 2S albumins isoforms from *Moringa oleifera* (AHG99681.1; AHG99682.1; AHG99683.1 and AHG99684.1), 2S storage protein 5-like from *Carica papaya* (XP_021906585.1), Mabinlin and Mabinlin II from *Capparis masaikai* (P30233.3 and BAA12204.1), 2S storage protein-5 from *Tarenaya hassleriana* (XP_010539281.1), 2S storage protein 1-like from *Carica papaya* (XP_021892915.1) and Mabinlins isoforms from *Capparis masaikai* (AAB31596.1; AAB31598.1; AAB31600.1; AAB25170.1 and 2DS2_A). The box indicates the sequence determined by homology.

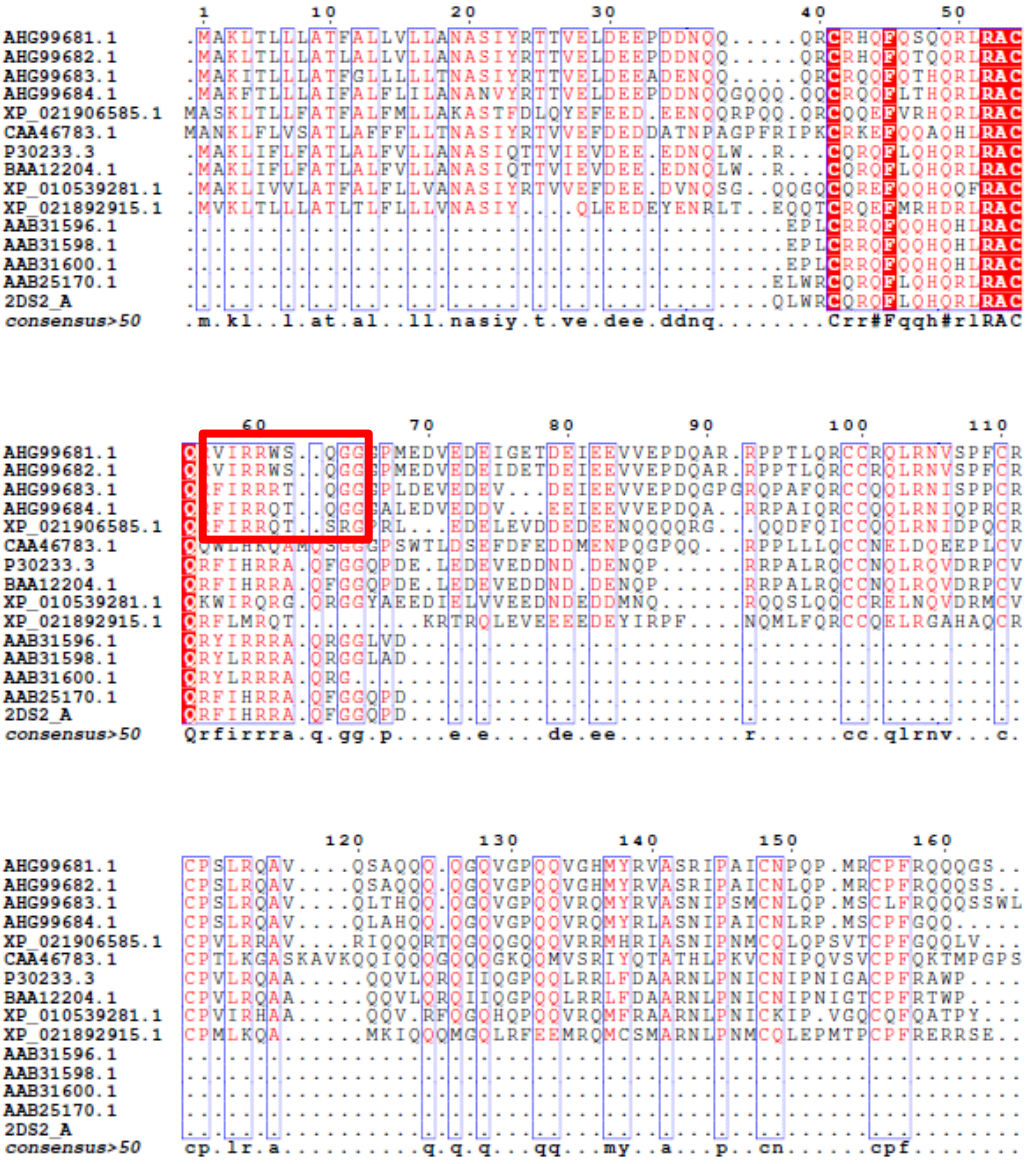

Source: prepared by the author.

Figure 3 - Photomicrograph of crystals from *Mo*-CBP_4 (~500 µm).

Source: prepared by the author.
Mo-CBP_4 (50 mg/mL) was solubilized in 0.02 M sodium acetate at pH 4.6 with 0.1 M NaCl. The crystals were screened at room temperature (± 25°C) in vapor-diffusion 24-well Linbro cell-culture plates.

Figure 4 - Overall structure of *Mo*-CBP$_4$ in an asymmetric unit.

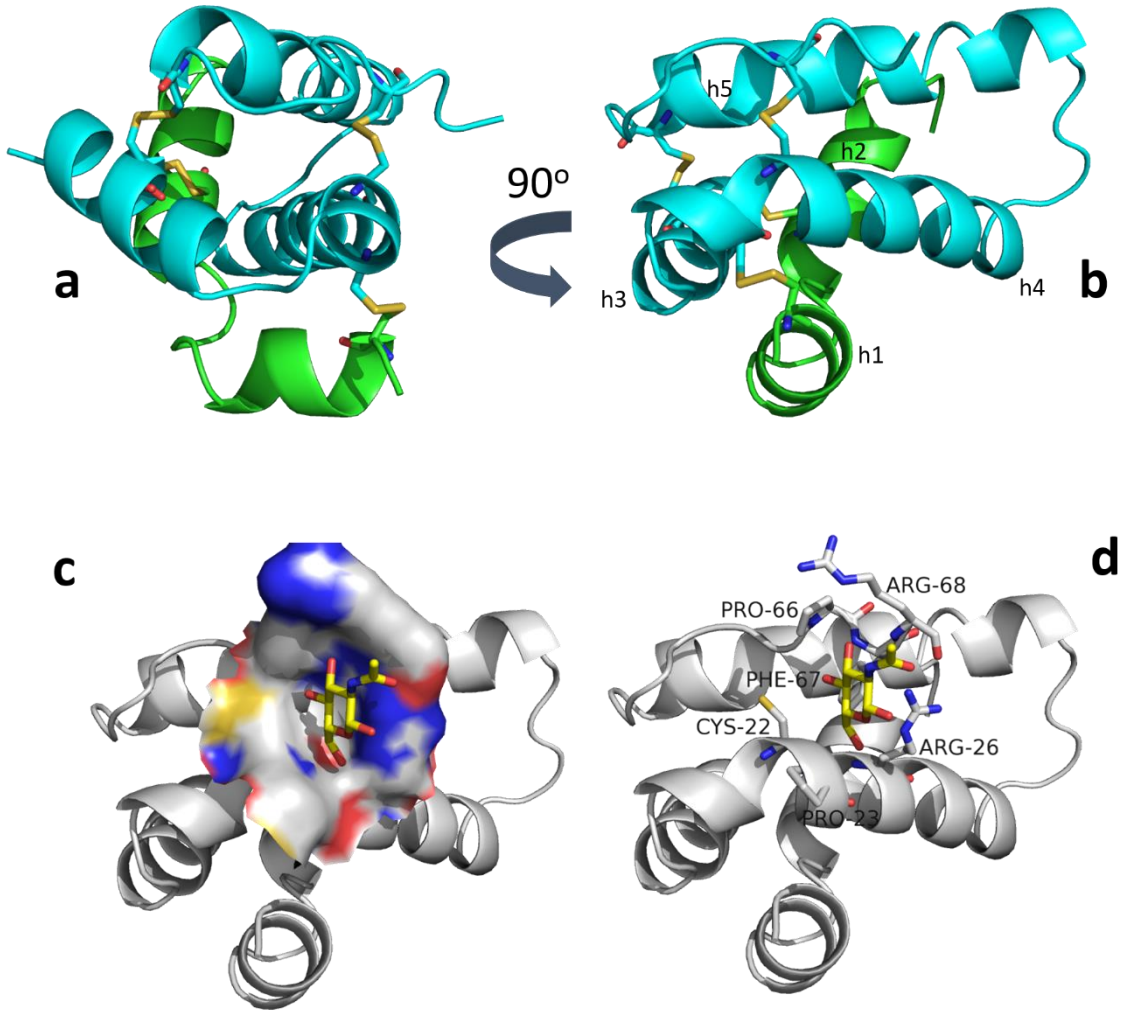

Source: prepared by the author.
(a-b) Ribbon presentation of *Mo*-CBP$_4$ molecule with the light and heavy chains represented in green and cyan respectively, and the cys-bonds in yellow details. (c) The surface drawing of the GlcNAc pocket and in (d) the six residues of the binding site arrangement.

Table 1 - Data collection and refinement statistics of *Mo*-CBP$_4$

DATA COLLECTION	
Source	LNLS
Wavelength (Å)	1.450
Resolution (Å)	39.87– 1.90 (1.94 - 1.90)
Space group	$I4_122$
Unit cell (Å)	a = b = 107.05, c = 42.96
Molecules / a.u.	1
Unique reflections	10152 (641)
Completeness (%)	100.0 (100.0)
R_{meas} [b]	0.076 (1.758)
R_{pim} [c]	0.021 (0.485)
R_{merge}	0.073 (1.688)
CC(1/2)	1.000 (0.837)
Multiplicity	24.6 (3.5)
I/sig(I)	31.0 (24.2)
B_{Wilson} (Å^2)	33.9
Software used for integration	XDS
Software used for scaling	Aimless
DATA REFINEMENT	
R_{cryst} [d]/ R_{free} [e]	0.198/ 0.227
No. Reflections used for R_{free} (%)	5
R.m.s.d. bonds (Å)	0.017
R.m.s.d. angles (º)	1.441
Software used for refinement	PHENIX refine
Refinement method	ML/TLS

Source: prepared by the author.

[a] Values in parentheses are for the highest resolution shell.

[b] $$R_{meas} = \frac{\sum_h \sqrt{\frac{n_h}{n_h - 1}} \sum_i^{n_h} \left| \hat{I}_h - I_{h,i} \right|}{\sum_h \sum_i^{n_h} I_{h,i}} \text{ with } \hat{I}_h = \frac{1}{n_h} \sum_i^{n_h} I_{h,i}$$

[c] $$R_{pim} = \sum_{hkl} \sqrt{\frac{1}{N-1}} \sum_i \left| I_i(hkl) - \overline{I(hkl)} \right| / \sum_{hkl} \sum_i I_i(hkl)$$

Where I (hkl) is the mean intensity of multiple I_i (*hkl*) observations of the symmetry-related reflections, N is the redundancy, n_h is the multiplicity, $\hat{I}_h$ is the average intensity and $I_{h,i}$ is the observed intensity.

[d] $R_{cryst} = \Sigma \, |F_o - F_c| \, / \, \Sigma \, F_o$

[e] R_{free} is the cross-validation R_{factor} computed for the test set of reflections (5 %) which are omitted in the refinement process.

5.3.3 N-Acetylglucosamine molecular docking

As first step, the “blind docking” approach was used in order to identify the potential fixation sites of GlcNAc. The resulting conformations of ligands were clustered (RMSD 2 Å) and most of them were found to be in a cleft region (Fig. 4c, d) between C-terminus and helix 3 heavy chain. The ligand was re-docked restraining the searching grid to this cleft obtaining a solution with an estimated free biding energy of -4.06 kcal/mol. The most important residues involved in the interaction with GlcNAc are those from the heavy chain, corresponding to Cys22, Pro23, Arg26, Pro66, Phe67, Arg68 (Fig. 5c). These residues are completely conserved in relation to *Mo*-CBP$_3$ (Fig. 5a, d).

Figure 5 - Sequence conserved between *Mo*-CBP$_4$ and *Mo*-CBP$_3$

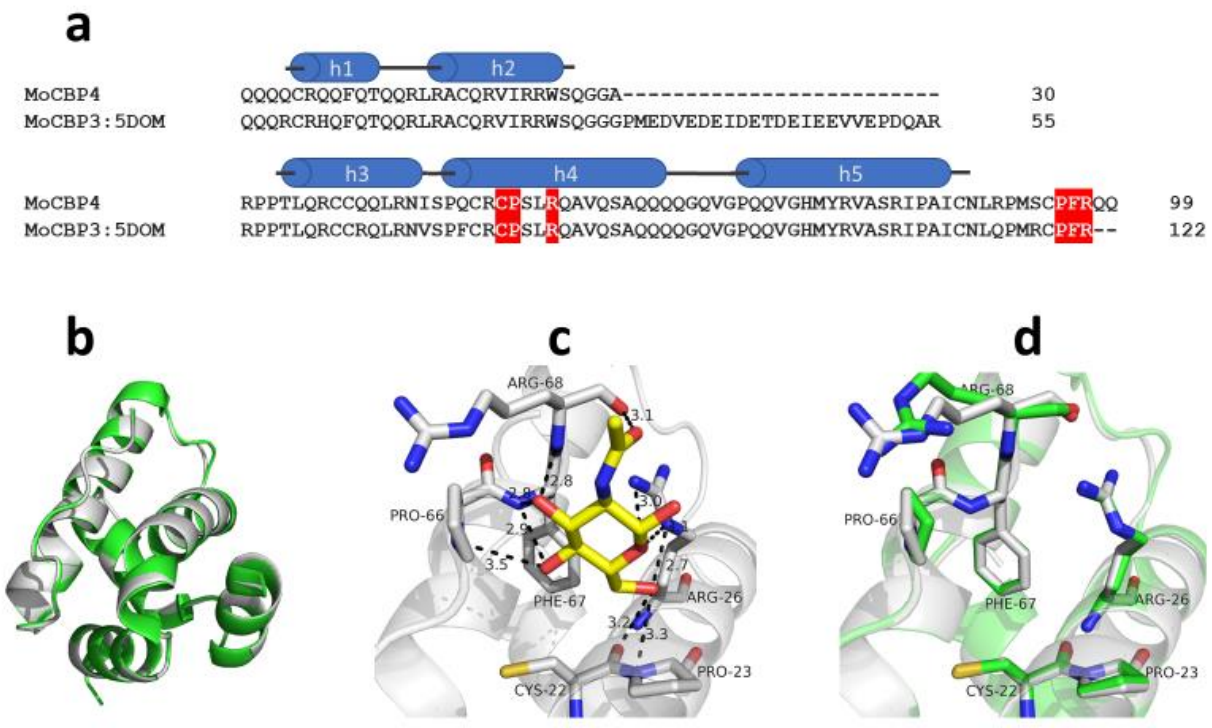

Source: prepared by the author.
(a) Sequence conserved between *Mo*-CBP$_4$ and *Mo*-CBP$_3$ shown conserved in potential binding with GlcNAc (highlighted in red). (b) *Mo*-CBP$_4$ (grey) and *Mo*-CBP$_3$ (green) superimposition shown similarity in sequence and structure (RMSD 0.115), (c) The potential binding site residues to GlcNAc (shown in yellow), and (d) its similarity to *Mo*-CBP$_3$.

5.3.4 Indirect Hemagglutinating activity

Mo-CBP$_4$ when bound to the anti-*Mo*-CBP$_4$ antibodies was able to agglutinate rabbit erythrocytes both treated and not treated with proteolytic enzymes. Hemagglutinating activity towards native and enzyme-treated rabbit erythrocytes was fully inhibited by N-acetyl-D-glucosamine (50 mM), but not by as much as D-glucose and D-mannose (50 mM).

5.3.5 Biological activities

Intraperitoneal administration of zymosan A (Zy) significantly increased the neutrophil migration to peritoneal cavity when compared to normal control group (Sal). As expected, the standard drug dexamethasone pretreatment (Dex) reduced intensely (83.5%) the neutrophils influx. The animals pretreated with *Mo*-CBP$_4$ at doses of 10 and 20 mg/kg did not show any beneficial effect (data not shown). However, at the highest dose (40 mg/kg) the protein drastically decreased the neutrophils count in the peritoneal cavity (47.8%) in relation to Zy group (Fig. 6). The noted effect of *Mo*-CBP$_4$ (40 mg/kg) on the neutrophils influx was completely abolished when protein was incubated with N-acetyl-D-glucosamine (GlcNAc) (Fig. 6). Interestingly, even after heat treatment at 100 °C/1 h, *Mo*-CBP$_4$ (40 mg/kg) preserved the anti-inflammatory activity with reduction by 48.3% in the neutrophils count (Fig. 6).

Intraperitoneal injection of zymosan A induced a significant release of TNF-α and IL-1β in the serum when compared to normal control (saline). The pretreatment with *Mo*-CBP$_4$ (40 mg/kg) 1 h before zymosan A injection was not able to alter TNF-α levels, however the protein decreased the release IL-1β (Fig. 7a, b). Regarding anti-inflammatory cytokine IL-10, the pretreatment with *Mo*-CBP$_4$ (40 mg/kg) was able to significantly amplify the IL-10 levels in the serum (Fig. 7c).

Figure 6 - *Mo*-CBP$_4$ inhibits zymosan A-induced neutrophil migration to peritoneal cavity.

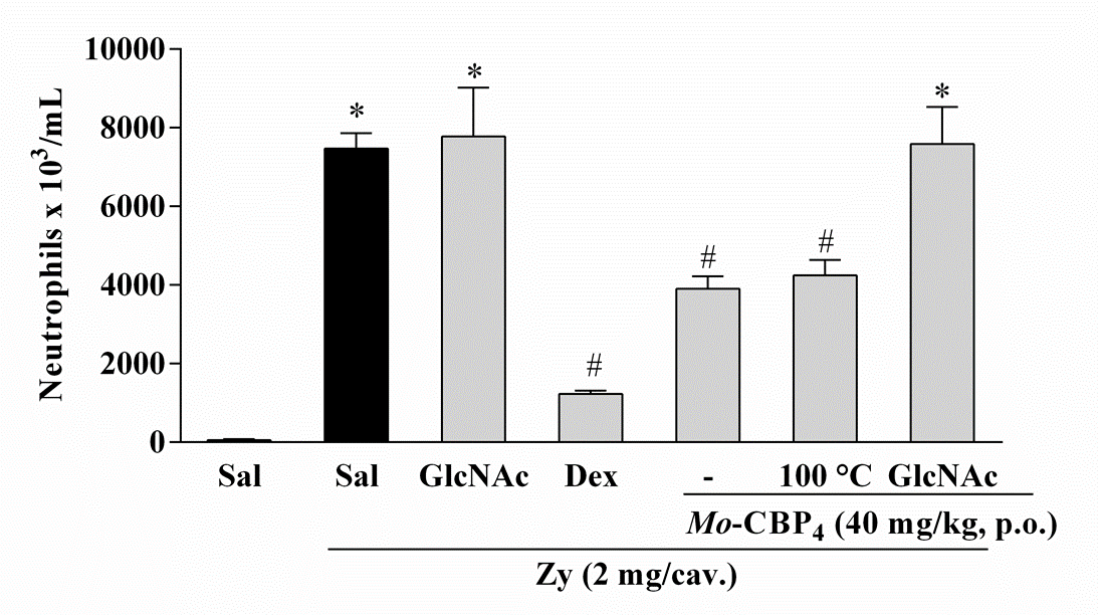

Source: prepared by the author.
This activity is heat-stable and sugar-binding dependent. Mice were treated 1h before zymosan (Zy; 2 mg; 200 µL saline/cavity; i.p) with *Mo*-CBP$_4$ (40 mg/kg; 200µL saline; p.o.), heated at 100 °C or combined with N-Acetylglucosamine (GlcNAc; 0.1 M; 200 µL saline; p.o.). Saline (sterile saline 0.9%; p.o.), Dexamethasone (Dex; 5 mg/kg; i.p.) or GlcNAc (0.1 M; 200 µL saline; p.o.) were used as control groups. Neutrophil count was evaluated after 4 h. Results are shown as the mean ± S.E.M. (n=5). *P < 0.05 compared to saline and #P < 0.05 compared to zymosan (ANOVA followed by Bonferroni's post test).

Figure 7 - Modulation of *Mo*-CBP$_4$ upon pro and anti-inflammatory cytokines in Zy-induced inflammation.

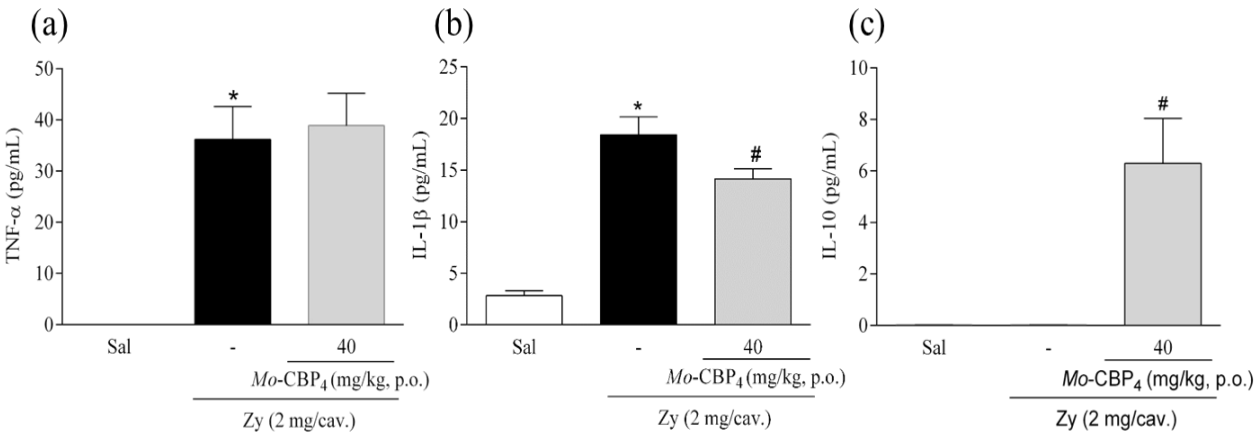

Source: prepared by the author.
Mice were treated 1h before Zy (2 mg; 200µL saline/cavity; i.p) with saline (Sterile saline 0.9%; p.o.) or *Mo*-CBP$_4$ (40 mg/kg; 200µL saline; p.o.). Serum was collected 4 h after Zy injection and used to measure levels of TNF-α (a), IL-1β (b) and IL-10 (c). Results are shown as the mean ±S.E.M. (n=8). *P < 0.05 compared to saline and #P < 0.05 compared to zymosan (ANOVA followed by Bonferroni's post test).

Carrageenan significantly induced mechanical hypernociception on the evaluated time points (1, 3 and 5 h) when compared with normal control group. As expected, mice treated with indomethacin (standard drug) were more resistant against the pressure on the paw when compared with Cg-group, showing significant anti-hypernociceptive effect. The pretreatment with *Mo*-CBP$_4$ at dose 40 mg/kg reduced (31%, 18% and 30% respectively) the mechanical hypernociception all time points analyzed (Fig. 8a).

Myeloperoxidase (MPO) activity in the plantar tissue was investigated to understand mode of action of anti-hypernociceptive activity of *Mo*-CBP$_4$. The protein at dose 40 mg/kg abolished drastically (96.0%) the neutrophil influx to plantar tissue when compared to Cg-group (Fig. 8b).

Figure 8 - *Mo*-CBP$_4$ attenuates Cg-induced mechanical hypernociception with reduction of MPO activity in the paw tissue.

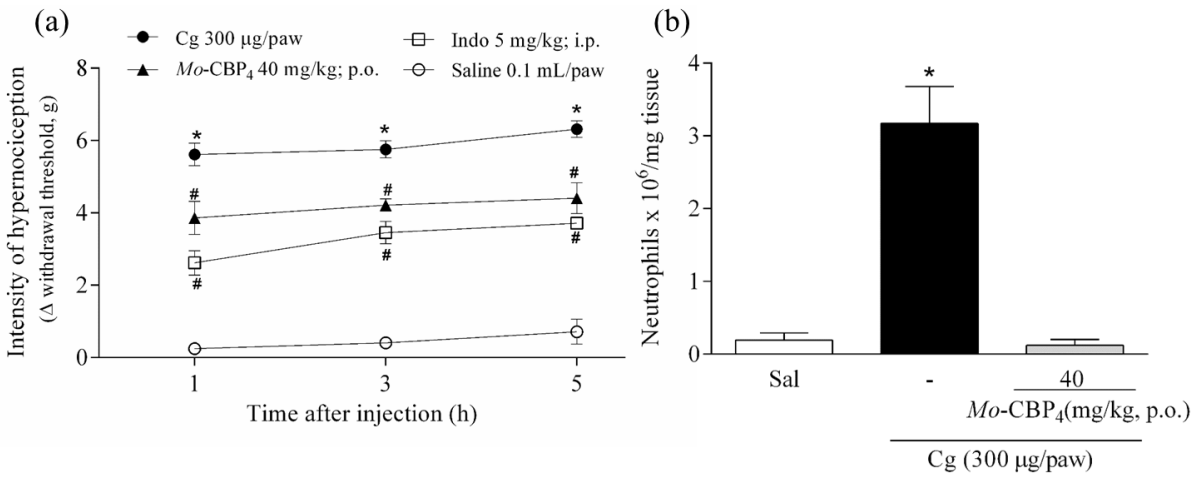

Source: prepared by the author.
Mice were treated 1 h before Cg (300 µg/50 µL saline/paw) with *Mo*-CBP$_4$ (40 mg/kg; 200 µL saline; p.o.), indomethacin (5 mg/kg; i.p.) or saline (i.pl.; i.v.). Hypernociceptive response was evaluated 1, 3 and 5 h after Cg injection (a). Plantar paw skin samples were collected 3 h after Cg injection and used to measure MPO activity (b). Results are shown as the mean ± S.E.M. (n=6). *P < 0.05 compared to saline and #P < 0.05 compared to Cg (ANOVA followed by Bonferroni's post test).

5.4 Discussion

The *Mo*-CBP$_4$ sequence was similar to several proteins of the 2S albumin class from *M. oleifera* and other species (Fig. 2). 2S albumin is a stock function protein found in plant seeds. They generally have low molecular weight (12-15 kDa) and are composed of two different polypeptide chains linked by disulfide bridges. The main feature of the amino acid sequence of these proteins is the distribution of their 8 cysteine residues in a conserved pattern (...C...C.../...CC...CXC...C...C). In addition, there are two more intra-chain bridges that confer stability to these proteins (PANTOJA-UCEDA et al., 2002). A remarkably similar pattern to that was found in *Mo*-CBP$_4$ (Fig. 5).

In addition to the amino acid sequence, *Mo*-CBP$_4$ also presented three-dimensional characteristics similar to *Mo*-CBP$_3$, a 2S albumin isolated from *M. oleifera* seeds, which was used as a model for refinement. The *Mo*-CBP$_4$ molecule consists of two polypeptide subunits, the light and heavy chains. The secondary structure consists of five helices labeled H1 to H5, connected by short loops. This structure is stabilized by two disulfide bridges between the two chains and by two intra-chain disulfide bridges (ULLAH et al., 2015; FREIRE et al., 2015). Like *Mo*-CBP$_4$, Mabinlin II isolated from the mature seeds of *Capparis masaikai* consisting of two covalent-linked polypeptide chains. These two chains are crosslinked by two inter-chain disulfide bridges. In addition, there is also two intra-chain disulfide bridges. The structure displays five α-helices (ULLAH et al., 2015; JIANG et al., 2008).

The *Mo*-CBP$_4$ structure shows some differences when compared to other chitin-binding lectins, such as those isolated from *Hevea brasiliensis* latex (Hevein) and *Urtica dioica* rhizomes (UDA). Hevein presents a central β-sheet with antiparallel β-strands surrounded by two small helices that are stabilized by four disulfide bridges (HOLLE; VAN DAMME, 2015; BERTHELOT; PERUCH; LECOMTE, 2016). UDA is a complex mixture of several isolectins, six of which have been isolated. Among these isolectins, UDA-VI consists of two domains: the N-terminal domain (domain-1) and the C-terminal domain (domain-2), both presenting four disulfide bonds. Two short β-strands form an antiparallel sheet structure in domain-1 and the corresponding β-strands in domain-2 (HARATA; MURAKI, 2000; SAUL et al., 2000).

There are some reports in the literature of lectins or lectin-like proteins that have been isolated from albumin fractions. For example, lectin isolated from *Crotalaria*

retusa and lectin-like protein isolated from *Acacia farnesiana*. However, Mo-CBP$_4$ is probably the first report of a 2S albumin with the characteristics of a lectin (ARAGÃO et al., 2017; SANTI-GADELHA et al., 2008; ABRANTES et al., 2013).

Molecular docking results demonstrate that *Mo*-CBP$_4$ can bind to GlcNAc. These results corroborate with one of the protein purification steps that uses affinity chromatography with a chitin matrix (polymer of GlcNAc). They also support the results of the hemagglutinating activity, which was inhibited when *Mo*-CBP$_4$ + antibody complex was pre-incubated with GlcNAc. In previous studies, it was found that *Mo*-CBP$_4$ was not able to agglutinate human or rabbit erythrocytes (PEREIRA et al., 2011). However, in our studies we demonstrated that *Mo*-CBP$_4$ showed indirect hemagglutinating activity via antibody. This indicates that this protein has just a single binding site for carbohydrate and thus constitutes a merolectin (VAN DAMME et al., 1998; PEUMANS; VAN DAMME, 1995). An important chitin-binding merolectin already reported in the literature is hevein (MISHRA et al., 2019). The binding of the lectin with GlcNAc can contribute to the biological activities of *Mo*-CBP$_4$, such as inflammation. GlcNAc can be found in glycoconjugates and are involved in many processes of cell-cell recognition, such as leukocyte recruitment (ALENCAR et al., 1999).

Neutrophils play an important role in the inflammation process. In order for these to migrate to the infection sites, selectins (endogenous lectins) come into action, interacting with the carbohydrates or glycoconjugates of the leukocytes, adhering them to the vascular endothelium. This process is especially important for the neutrophil to pass to the inflammation site (ROSALES, 2018; NÉMETH; SPERANDIO; MÓCSAI, 2020; Mortaz et al., 2018). It´s possible that *Mo*-CBP$_4$ is able to reduce the inflammatory process by inhibiting the neutrophil-endothelium interaction, competing or blocking the neutrophil-binding carbohydrates common to selectins. Like the chitin-binding lectin isolated from *Lonchocarpus sericeus*, *Mo*-CBP$_4$ had its anti-inflammatory activity reversed when pre-incubated with GlcNAc, showing the dependence of the carbohydrate interaction domain in the leukocyte migration inhibition process (NAPIMOGA et al., 2007). Other lectins also had their anti-inflammatory activity inhibited when they were pre-incubated with their respective specific carbohydrates (MOTA et al., 2006; ALENCAR et al., 2010; FIGUEIREDO et al., 2009). *Mo*-CBP$_4$ was also able to preserve its anti-inflammatory activity even though it was preheated to 100 ° C for 1 hour, result that corroborates with the high stability found in its structure through the disulfide bridges.

Another approach used to study the mode of action of *Mo*-CBP$_4$ was to evaluate its effect on the release of pro- and anti-inflammatory cytokines. TNF-α and IL-1β cytokines are pro-inflammatory and induce neutrophil migration (FIGUEIREDO et al., 2009; FELDMANN; PUSEY, 2006). *Mo*-CBP$_4$ was able to interfere only with the levels of IL-1β in the serum of animals, causing its reduction. Other lectins also influenced the release of IL-1β in models of acute inflammation. For example, *Canavalia grandiflora* agglutinin, in zymosan-induced peritonitis, reduced the levels of this cytokine in the peritoneal fluid and the *L. sericeus* chitin-binding lectin which reduced the levels of IL-1β and TNF-α in a peritonitis model and paw edema (NAPIMOGA et al., 2007; NUNES et al., 2009). In addition, *Mo*-CBP$_4$ was able to increase the levels of IL-10 in the animals' serum. IL-10 is an anti-inflammatory cytokine that controls the inflammatory process by suppressing the expression of proinflammatory cytokines, chemokines, adhesion molecules, as well as antigen-presenting and costimulatory molecules in monocytes/macrophages, neutrophils, and T cells [58–60]. (SARAIVA; VIEIRA; O'GARRA, 2019; ASADULLAH; STERRY; VOLK, 2003; SULTANI et al., 2012).

Regarding the nociception tests, the results showed that *Mo*-CBP$_4$ was able to inhibit the sensitization caused by carrageenan in the three times tested. The performance of the protein was very similar to that of indomethacin which is a standard analgesic and anti-inflammatory drug for this test. It has been reported in the literature that neutrophils are essential for the release of chemical mediators that will act directly in the sensitization of nociceptors (CUNHA et al., 2008; FRANCHIN et al., 2012; RIBEIRO et al., 2019). Therefore, it was investigated whether the anti-hypernociceptive activity of *Mo*-CBP$_4$ would be related to inhibition of neutrophil migration. For this, the enzyme myeloperoxidase (MPO) was dosed, which is a protein found in the neutrophil granules. This dosage provides an indirect quantification of these cells that have migrated to the inflammation site. The results showed that *Mo*-CBP$_4$ was able to inhibit the migration of neutrophils, indicating its relationship with the anti-hypernociceptive activity of the protein (CUNHA et al., 2005).

5.5 Conclusion

This work reported on the primary and tertiary structure of a lectin purified from *Moringa oleifera* seeds. *Mo*-CBP$_4$ is structurally similar to proteins of the 2S albumin class presenting an important anti-inflammatory activity, decreasing neutrophil migration and modulating pro and anti-inflammatory cytokines in a model of peritonitis. Furthermore, *Mo*-CBP$_4$ is able to attenuate the mechanical hypernociception induced by carrageenan. The protein showed high affinity for GlcNAc, having its anti-inflammatory activity reversed when pre-incubated with carbohydrate. With the obtained results, it is likely that this lectin can be applied as a tool in studies of inflammation and hypernociception.

6 ARTIGO 2 REFERENTE À TESE

Título

Mo-CBP$_4$, a chitin-binding protein isolated from *Moringa oleifera* Lam seeds, facilitates cutaneous wound healing process

Autoria

Tiago Deiveson Pereira Lopes[a*], Tamiris de Fátima Goebel de Souza[b], Gisele de Fátima Pinheiro Rangel[b], Janaina Serra Azul Monteiro Evangelista[c], José Tadeu Abreu Oliveira[a], Ilka Maria Vasconcelos[a], Nylane Maria Nunes de Alencar[b], Daniele de Oliveira Bezerra de Sousa[a *]

[a] Department of Biochemistry and Molecular Biology, Federal University of Ceará, Fortaleza, Ceará, Brazil

[b] Department of Physiology and Pharmacology, Federal University of Ceará, Fortaleza, Ceará, Brazil

[c] Histology Laboratory, University of the State of Ceará, Fortaleza, Ceará, Brazil

[*] Corresponding authors. E-mail address: t.deiveson@gmail.com (LOPES, T. D. P.) and daniele.sousa@ufc.br (SOUSA, D.O.B.)

ABSTRACT

Due to the high cost and limitations of current cutaneous wound healing treatments, the search for alternative approaches or medications, especially medicinal plants, has gained a lot of importance. In this study, we report wound healing activities of *Mo*-CBP$_4$, a chitin-binding protein isolated from seeds of *Moringa oleifera* Lam. *Mo*-CBP$_4$ was purified after protein extraction with 50 mM Tris-HCl buffer, pH 8.0, and chromatography on chitin and CM Sepharose™ columns. The results showed that *Mo*-CBP$_4$ had no cytotoxic effect on L929 fibroblasts in the tested concentration range, on the contrary, it had a proliferative effect. *Mo*-CBP$_4$ showed a stimulatory effect on the proliferation and migration of fibroblasts in scratch assay and effectively promoted wound closure in mouse model without causing body weight loss. The protein was also able to increase the levels of transforming growth factor (TGF-β) and vascular endothelial growth factor (VEGF) in L929 fibroblasts culture. *Mo*-CBP$_4$ treatment prevented a prolonged inflammatory process by regulating pro-inflammatory cytokines including interleukin (IL) -1β and tumor necrosis factor-α (TNF-α), and anti-inflammatory cytokine interleukin (IL) -10. These findings may enable the utilization of *Mo*-CBP$_4$ as a potent therapeutic for cutaneous wound healing.

Keywords: Cutaneous wound. Chitin-binding protein. *Moringa oleifera.* Wound healing effect.

6.1 Introduction

The skin is an important organ, functioning as a protective barrier against physical damage, fluid loss and invasion of toxic substances. In case of damage, the integrity of the skin must be restored as soon as possible (PENN; GROBBELAAR; ROLFE, 2012; SABOL et al., 2012; NGUYEN et al., 2017). These lesions, in which the skin is torn, cut or punctured, resulting in loss of epithelial integrity accompanied by disruption of the normal structure and function of the skin and its underlying tissue, are called cutaneous wounds (FRIEDMAN, 2011; YARISWAMY et al., 2013; NGUYEN et al., 2017). Wounds can occur as part of a disease process or have an accidental origin, mainly due to a chemical, microbial, physical or thermal injury, occurring on the surface of the skin or mucous membranes, or on organic tissues (JOSHI et al., 2016; SINGH; YOUNG, MCNAUGHT, 2017; ABDUL-NASIR-DEEN et al., 2020).

Cutaneous wounds are of public health interest and are currently considered a very challenging pathological problem, since reduce patient life quality, leading to extended hospitalization time and accounting for significant amount of healthcare expenditures. Chronic wounds cause pain, loss of function and mobility, and even negative psychological impact such as depression and anxiety. In addition, wounds can cause diseases and abnormalities that damage the skin tissue of infected individuals. It is estimated that, about 6 million people are battling with chronic wounds (AGYARE et al., 2009; PEREIRA et al., 2016; BOAKYE et al., 2018; ABDUL-NASIR-DEEN et al., 2020). Several types of treatment have already been developed to quickly achieve the closure of skin wounds, which include antibacterial ointments containing enzymatic substances (DNAse and collagenase), synthetic growth factors, polyurethane, hyaluronic acid hydrogels and dressings. Numerous wound dressings have been developed, however, ideal healing characteristics such as efficacy in absorbing exudates, flexibility, durability, adherence and low cost have not yet been fully achieved (MURAKAMI et al., 2010; PEREIRA et al., 2016). Wound healing is a clinical problem, requiring the development of new approaches for acute and chronic wound management. Therefore, a better understanding of the biological process involved in wound healing and tissue regeneration is essential.

The wound healing process is a dynamic and complex mechanism formed by the phases of hemostasis, inflammation, proliferation and remodeling. The process involves several cell types, such as neutrophils, macrophages, lymphocytes,

keratinocytes, fibroblasts and endothelial cells, and is coordinated by a signaling system involving various growth factors, cytokines and chemokines (JOSHI et al., 2016; AQUINO et al., 2019). The inflammation phase is critical to the healing process, activating the innate immune system, which protects humans from the invasion of pathogens and helps to remove necrotic tissue. During this phase, inflammatory cells, inflammatory factors and growth factors are secreted to coordinate the healing process (SUI et al., 2020). However, if the inflammatory response is elongated or exacerbated, it leads to a delay in the subsequent phases of proper wound healing. Therefore, inhibition of inflammation has a very important impact on wound healing as it facilitates the transition from the wound to the subsequent proliferative phase. In addition, fibroblast proliferation and migration are also very important for the wound healing process (LI et al., 2015; NGUYEN et al., 2017).

With this, studies in search of substances with healing activity have been stimulated, with substances derived from natural sources receiving great prominence. Plants have an immense potential for the management and treatment of wounds (YARISWAMY et al., 2013; AQUINO et al., 2019; ABDUL-NASIR-DEEN et al., 2020). There are several reports of plants that exhibited antimicrobial and anti-inflammatory properties that were essential to the wound healing process (EZZAT; CHOUCRY; KANDIL, 2016; DEV et al., 2019; USTUNER et al., 2019). In this context, the plant species *Moringa oleifera* Lam. is presented. *M. oleifera* (Family: Moringaceae) is a species native from Northeast India, which is largely used due to its therapeutic properties. For example, several studies have cited *M. oleifera* for having anti-inflammatory, anti-tumor, antioxidant, antidiabetic and antimicrobial properties (CHIN et al., 2018; PADAYACHEE; BAIJNATH, 2020; CRETELLA et al., 2020). *M. oleifera* is also widely used in the treatment of skin wounds and there are already several research studies on its wound healing activity. Studies with the extract of leaves and seeds showed the use of this species in the treatment of skin wounds (HUKKERI et al., 2006; RAWAT et al., 2012; BHATNAGAR et al., 2013; SIVARANJANI; PHILOMINATHAN, 2016; MUHAMMAD et al., 2016).

Focused on clinical trials our research group has been seeking proteins from *M. oleifera* who present healing potential of skin wounds. In this study, we reported the healing activity of *Mo*-CBP$_4$, a chitin-binding protein purified from *M. oleifera* seeds. *Mo*-CBP$_4$ is a basic protein (pI 10.55), the molecular mass of 11.78 kDa and potent antinociceptive and anti-inflammatory activity both administered orally and

intraperitoneally. *Mo*-CBP$_4$ also showed antimicrobial activity, exhibiting antifungal effect against the dermatophyte fungus *Trichophyton mentagrophytes* (PEREIRA et al., 2011; LOPES et al., 2020). Since *Mo*-CBP$_4$ exhibits anti-inflammatory and antimicrobial activity, it is likely that this compound could promote wound healing. Herein, we tested whether *Mo*-CBP$_4$ could promote wound healing in a murine mouse model and fibroblasts proliferation and migration in an in vitro assay. In addition, we measured levels of cytokine protein and growth factors, including tumor necrosis factor-α (TNF-α), interleukin (IL) −1β, IL-10, transforming growth factor (TGF-β) and vascular endothelial growth factor (VEGF).

6.2 Materials and methods

6.2.1 Plant material

Moringa oleifera seeds were collected from trees at the Pici Campus of Federal University of Ceará (UFC), Fortaleza, Brazil. A voucher specimen (No. EAC34591) was deposited at the Prisco Bezerra Herbarium, UFC.

6.2.2 Protein extraction and purification

Purification of *Mo*-CBP$_4$ was performed following protocol described by Lopes *et al*. (2020). Mature seeds were ground in a coffee grinder and treated with n-hexane (1:10, w/v). Defatted flour was extracted with 50 mM Tris-HCl buffer, pH 8.0, containing 150 mM NaCl (1:10 w/v), for 4 h at 4 °C, filtered through cheesecloth and centrifugated at 15,000 x g, 4 °C, 30 min. Next, the supernatant was exhaustively dialyzed against distilled water and centrifuged under the same conditions. The soluble proteins (albumin fraction) resuspended in extraction buffer were submitted to affinity chromatography (chitin matrix) previously equilibrated with the above buffer. The *M. oleifera* chitin-binding proteins (*Mo*-CBPs) were eluted with 50 mM acetic acid, pooled, and dialyzed against distilled water at 4° C. *Mo*-CBPs fraction in 50 mM sodium acetate buffer, pH 5.2 was applied to a cation-exchange matrix (CM-Sepharose^{TM}) pre-equilibrated with the same buffer. The adsorbed proteins were eluted by stepwise method with increasing NaCl concentrations. *Mo*-CBP$_4$ (*Mo*: *M. oleifera*; CBP: Chitin-Binding Protein) corresponds as the peak eluted with 600 mM NaCl.

6.2.3 In vitro study

6.2.3.1 Cell culture

The mouse fibroblast cell line (L929 - ATCC®) was purchased from the Cell Bank of Rio de Janeiro, Brazil. The cells were cultured in Dulbecco's modified Eagle medium (DMEM, Gibco®) supplemented with 10% fetal bovine serum (FBS - Gibco®), 100 IU mL^{-1} penicillin and 100 µg mL^{-1} streptomycin (Gibco®) at 37 °C in a humidified atmosphere containing 5% CO_2.

6.2.3.2 Cell cytotoxicity test: SRB assay

In vitro cytotoxic activity was measured by the standard colorimetric sulforodamine B (SRB) assay (HOUGHTON et al., 2007). L929 cells were seeded at

a density of 2 x 10^4 cells in 96-well plates with 2.5% DMEM, followed by treatment with *Mo*-CBP4 (1.56, 3.12, 6.25, 12.5 and 25 µg/mL) and incubated for 24, 48 and 72 h. Negative control tests consisted of saline and/or DMEM (2.5%). At the end of incubation time, the culture medium was completely removed and 100 µL of 10% trichloroacetic acid (TCA) was added to each well and left at 4 °C for 1 h. Next, the TCA-fixed cells were stained with 100 µL of 0.4% (w/v) SRB in 1% acetic acid and kept in an incubator at 5% CO_2 and 37 ºC for 30 min. The plates were washed with 1% acetic acid and then added 200 µL of 10 mM Trizma base (Tris[hydroxymethyl]aminomethane). The absorbance of each well was recorded on a plate reader (Multiskan FC – Thermo Scientific®) at 570 nm. Cell survival was measured as the percentage absorbance compared to the control (non-treated cells).

6.2.3.3 Measurement of TGF-β and VEGF

L929 cells were seeded in 96-well plates (2 x 10^4 cells/mL) containing 2.5% DMEM, treated with *Mo*-CBP_4 (6.25, 12.5 and 25 µg/mL) and kept in an incubator at 5% CO_2 and 37 ºC for 48 h. As control tests we utilized saline and 2.5% DMEM (negative controls), and 10% DMEM as positive control. After the incubation period, Transforming Growth Factor (TGF-β) and Vascular endothelial growth factor (VEGF) levels from cell culture supernatants were measured by using the Mouse TGF-beta 1 DuoSet ELISA kit (R&D Systems - Catalog Number: DY1679) and Mouse VEGF DuoSet ELISA kit (R&D Systems - Catalog Number: DY493), respectively, according to the instruction of the manufacturer, The reading was performed in a microplate reader at a wavelength of 450 nm. The results were expressed as TGF-β and VEGF levels in pg per mL of cell culture supernatant (HORMOZI; ASSAEI; BOROUJENI, 2017; SCHERER et al., 2019).

6.2.3.4 Scratch wound healing assay

The effect of *Mo*-CBP_4 on L929 fibroblasts migration and proliferation was assessed using a scratch wound healing assay (KIM; KU; CHOI, 2020; RÄSÄNEM; VAHERI, 2010). Scratch wound analysis was performed in confluent monolayers of L929 cells. Initially, the cells were incubated with 0.1% trypsin for 20 min and then plated in 24-well plates at a density of 5 x10^4 cells per well, maintained in DMEM medium supplemented with 2.5% fetal bovine serum in a humidified atmosphere containing 5% CO_2 at 37°C for 48 h. A linear scratch was generated in the cell

monolayer using a sterile 200 µL plastic pipette tip, and the wells were washed with PBS to remove cell debris. Then, a new medium (DMEM 2.5%) was added. The cells were then treated with *Mo*-CBP$_4$ (6.25, 12.5 and 25 µg/mL). Images were obtained from the same fields immediately after scratching and after 12, 24, 48 and 72 h of incubation, using a microscope with a digital camera. The cell migration and proliferation rate were determined by measuring the reduction of the open area (cell-free) using TSCRACTH® software (GEBÄCK et al., 2009).

6.2.4 In vivo study

6.2.4.1 Biomembrane preparation

Initially, a 1% PVA solution was prepared using distilled water. After this, 1% PVA was mixed with *Mo*-CBP$_4$ (1% or 5%) to obtain the following final solutions: 1% PVA + 1% *Mo*-CBP$_4$ or 1% PVA + 5% *Mo*-CBP$_4$. These solutions were stirred at 50 ºC for 2 h. The resulting mixtures were filtered using a funnel with a sintered glass plate under vacuum and then poured into Petri plates (13.0 cm diameter/height 1.0 cm). The mixtures were dried in an air circulation oven at 40 ºC until the solvent was completely evaporated and then adequately protected to prevent contamination. The PVA membranes containing *Mo*-CBP$_4$ were named BioMem 1% or 5% PVA/M$_4$ (FIGUEIREDO *et al*., 2014).

6.2.4.2 Animals

Swiss mice, weighing 20-30 g, were provided by the Animal House of the Federal University of Ceará, Brazil. The animals were housed in groups of five in standard cages at room temperature (25 ± 3 °C) and exposed to a 12 h dark/12 h light cycle; both food and water were offered *ad libitum*. Twelve hours before experimentation, they were transferred to the laboratory and housed only with water *ad libitum*. The experimental protocols were performed in accordance with the current guidelines for the care of laboratory animals and the ethical guidelines for investigations of experimental pain in conscious animals, reviewed and approved by the Animal Ethics Committee of UFC, Brazil (protocol number: 86/10).

6.2.4.3 Wound-induced model

The mice were anesthetized by intraperitoneal injections of 10% ketamine hydrochloride (115 mg/kg) and 2% xylazine hydrochloride (10 mg/kg) before their

surgical procedure (HALL; CLARKE, 1991). After shaving the dorsal surface skin, the region was prepared for aseptic surgery using 1% iodopovidone, followed by 70% ethanol. Two circular excisional wounds with 1.0 cm^2 diameter were induced, with a surgical punch, on the dorsal surface of each animal. The excisional wounds were not sutured, so that the healing occurred by secondary intention. After the surgery, the animals received subcutaneously (s.c.) 1 mL of sterile 0.9% saline for fluid replacement and were kept in a warm environment until complete recovery from anesthesia (CARDOSO *et al*., 2007). They were randomly divided into 4 groups (n=10/group), as follows: animals subjected only to surgical procedures (Sham), animals treated with 1% polyvinyl alcohol membrane (Control), and animals treated with BioMem 1% or 5% PVA/M_4.

6.2.4.4 Macroscopic Analyses (Wound Area Measurements)

Macroscopic differences in neoformed tissue were monitored at the 2^{nd}, 5^{th}, 7^{th}, 9^{th} and 12^{th} days after surgery. For that, areas of excisional wounds in mm^2 were calculated with a pachymeter, as follows: $A = \pi \times R \times r$, where *A* is the area and *R* and *r* are large and small rays, respectively (PRATA *et al*., 1988). The results were expressed as percentage of wound area contraction. In addition to the measurement, the wounds were also photographed with a digital camera. After the macroscopic study, 5 mm punch biopsies from neoformed tissues and excisional wounds with adjacent normal skin were removed (n = 6/group) for histological study and cytokine measurement. Then, the animals were euthanised with an anaesthetic overdose (ketamine, 350 mg/kg, ip).

6.2.4.5 Histopathological Analyses

Neoformed tissues of excisional wounds were fixed in formaldehyde (10%, v/v) and resuspended in 0.01 M PBS (Phosphate-Buffered Saline), pH 7.2, over 24 hours, for histological processing. Sections (5 mm) were stained with Hematoxylin-Eosin (HE). Photomicrographs of sections were obtained, 2, 7 and 12 days after surgery, under a polarizing microscope.

6.2.4.6 Measurement of cytokines

Tissue samples were obtained on 2^{th} post-wounding day from excision wound model. The tissues (n = 6/group) were crushed and homogenized at 4ºC

(POLYTRON®) in PBS solution (pH 7.4) and centrifuged at 5000 rpm for 5 min to remove residues that were not completely crushed. The cytokines interleukin -1β (IL-1β), interleukin-10 (IL-10), tumor necrosis factor-α (TNF-α) were assessed by ELISA kit (R&D systems) using Mouse IL-1 beta/IL-1F2 DuoSet (Catalog Number: DY401), Mouse IL-10 DuoSet (Catalog Number: DY417) and Mouse TNF-alpha DuoSet (Catalog Number: DY410) in tissue homogenates obtained. The ELISA protocol was followed as per manufacturer guideline. The reading was performed in a microplate reader at a wavelength of 450 nm. The results were expressed as IL-1β, IL-10 and TNF-α levels in pg per mg of tissue (JOSHI et al., 2016; PEREIRA et al., 2016).

6.2.4.7 Statistical analysis

All results are expressed as mean values of groups ± SEM. Statistical evaluation was performed by analysis of variance (ANOVA) followed by Bonferroni's test. The level of significance was determined as $P < 0.05$, using the Graph Pad Prism, version 6.0.

6.3 Results

6.3.1 In vitro study

6.3.1.1 Cell cytotoxicity

Figure 9 reveals that *Mo*-CBP$_4$, in all doses tested, did not exhibit any cytotoxic effect against L929 fibroblasts. In contrast, proliferative effects were observed in L929 cells, which exhibited increased cell viability after 48 (Fig. 9b) and 72 h (Fig. 9c) of treatment with 1.56, 3.12, 6.25 and 12.5 µg/mL *Mo*-CBP$_4$.

6.3.1.2 TGF-β and VEGF measurement

Using ELISA analysis, an increase in the levels of TGF-β and VEGF growth factors was observed in the L929 fibroblasts culture supernatant treated with *Mo*-CBP$_4$ (6.25, 12.5 and 25 µg/mL). TGF-β levels increased when compared to negative controls (saline and 2.5% DMEM) (Fig. 10a), while VEGF levels increased compared to both negative and positive (10% DMEM) controls (Fig. 10b).

6.3.1.3 Scratch wound healing assay

The scratch assay mimics to some extent the migration of cells *in vivo*. *Mo*-CBP$_4$ (6.25, 12.5 and 25 µg/mL), after 24 h, significantly enhanced the proliferation

and migration of L929 fibroblasts decreasing the percentage of open area (cell-free) compared to saline (Fig. 11b). At 36 and 48 hours (Fig. 11c and d) of incubation, *Mo*-CBP_4 decreased the percentage of open area in relation to both negative controls (saline and 2.5% DMEM). The protein showed similar efficiency to the positive control (10% DMEM) at 36 h (25 µg/mL) and 48 h (12.5 and 25 µg/mL) of incubation. Figure 12 shows the photomicrographs produced by the TSCRATCH® software to assess the open area (cell-free).

Figure 9 - Cellular viability of L929 fibroblasts after of exposure to *Mo*-CBP$_4$

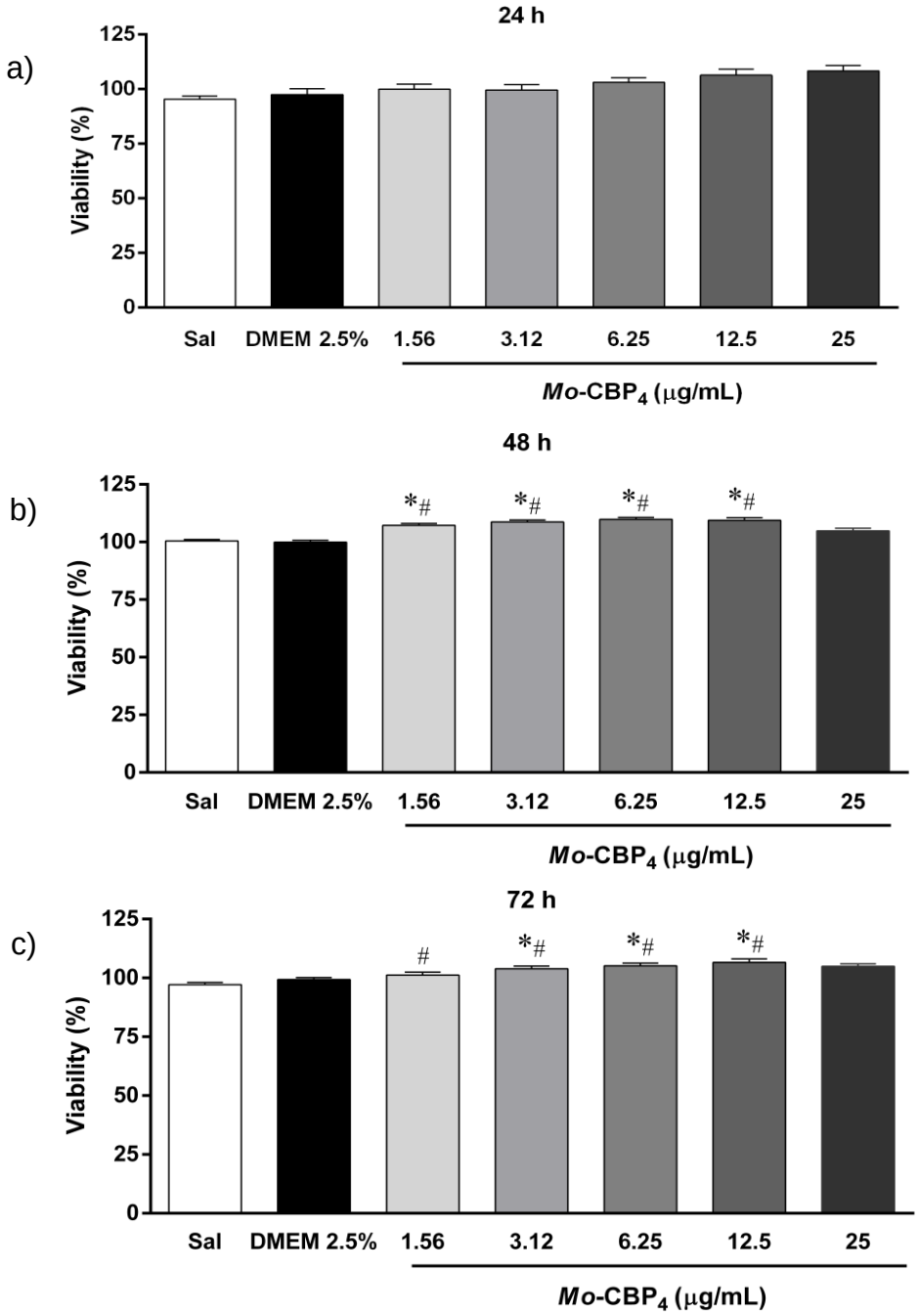

Source: prepared by the author.
Cellular viability of L929 fibroblasts after 24 (a), 48 (b) e 72 h (c) of exposure to *Mo*-CBP$_4$ (1.56 – 25 µg/mL), as determined by the colorimetric SRB assay. Values are expressed as the percentage of cellular viability compared to the controls and represent the means ± SD of three independent experiments (n=8). Saline and DMEM (2.5%) were used as negative control tests. *P < 0.05 compared to saline and $^{\#}$P < 0.05 compared to DMEM (2.5%) (ANOVA followed by Bonferroni's posttest).

Figure 10 - Dosage of growth factors in the supernatant of the L929 fibroblasts culture treated with *Mo*-CBP$_4$

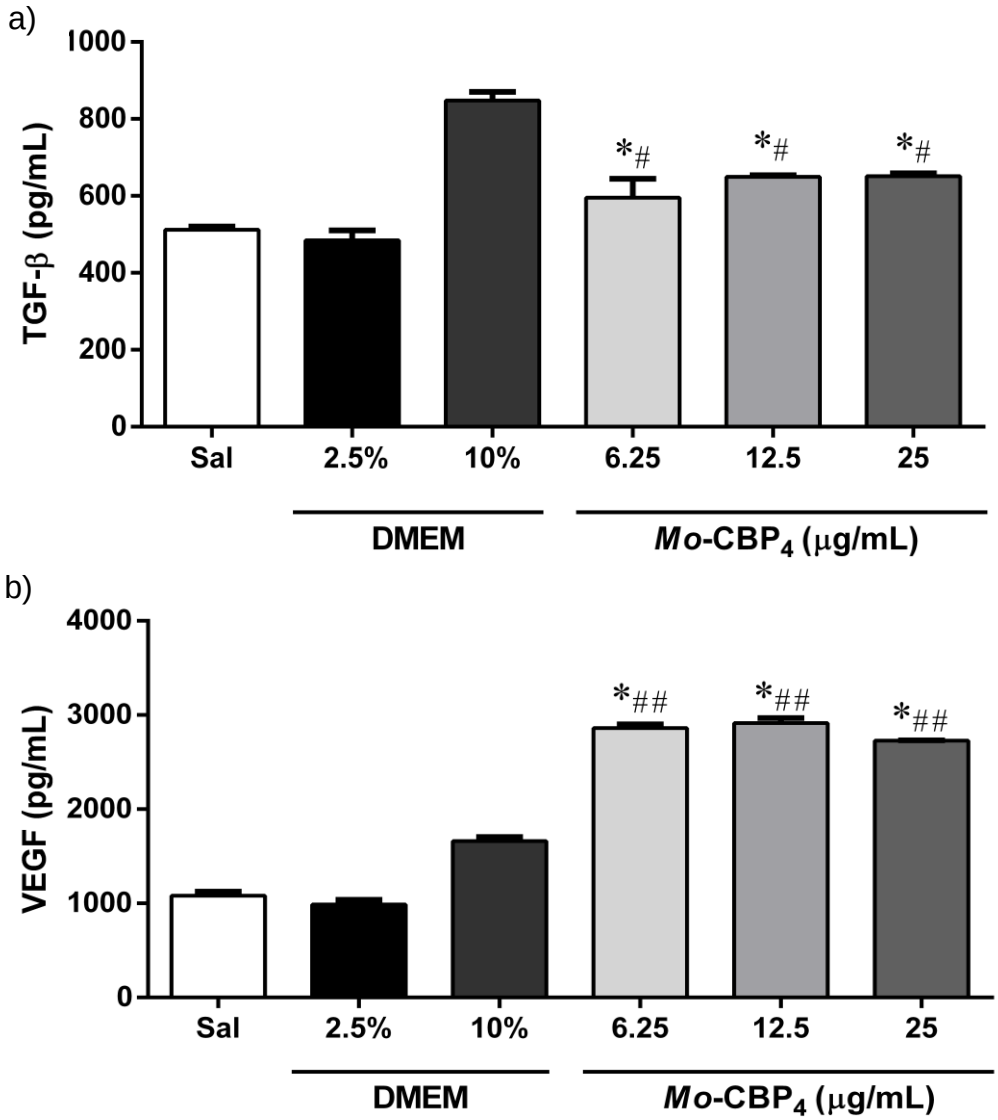

Source: prepared by the author.
Dosage of growth factors in the supernatant of the L929 fibroblasts culture treated with *Mo*-CBP$_4$ (6.25, 12.5 and 25 µg/mL), as determined by the ELISA assay. The results were expressed as TGF-β (a) and VEGF (b) levels in pg per mL of cell culture supernatant compared to the controls and represent the means ± SD of three independent experiments (n=4). Saline and DMEM (2.5%) were used as negative controls and DMEM (10%) as positive control. *P < 0.05 compared to saline, $^{\#}$P < 0.05 compared to DMEM (2.5%) and $^{\#\#}$P < 0.05 compared to DMEM (10%) (ANOVA followed by Bonferroni's posttest).

Figure 11 - Effect of *Mo*-CBP$_4$ on the proliferative and migratory activities of L929 fibroblasts in the scratch assay.

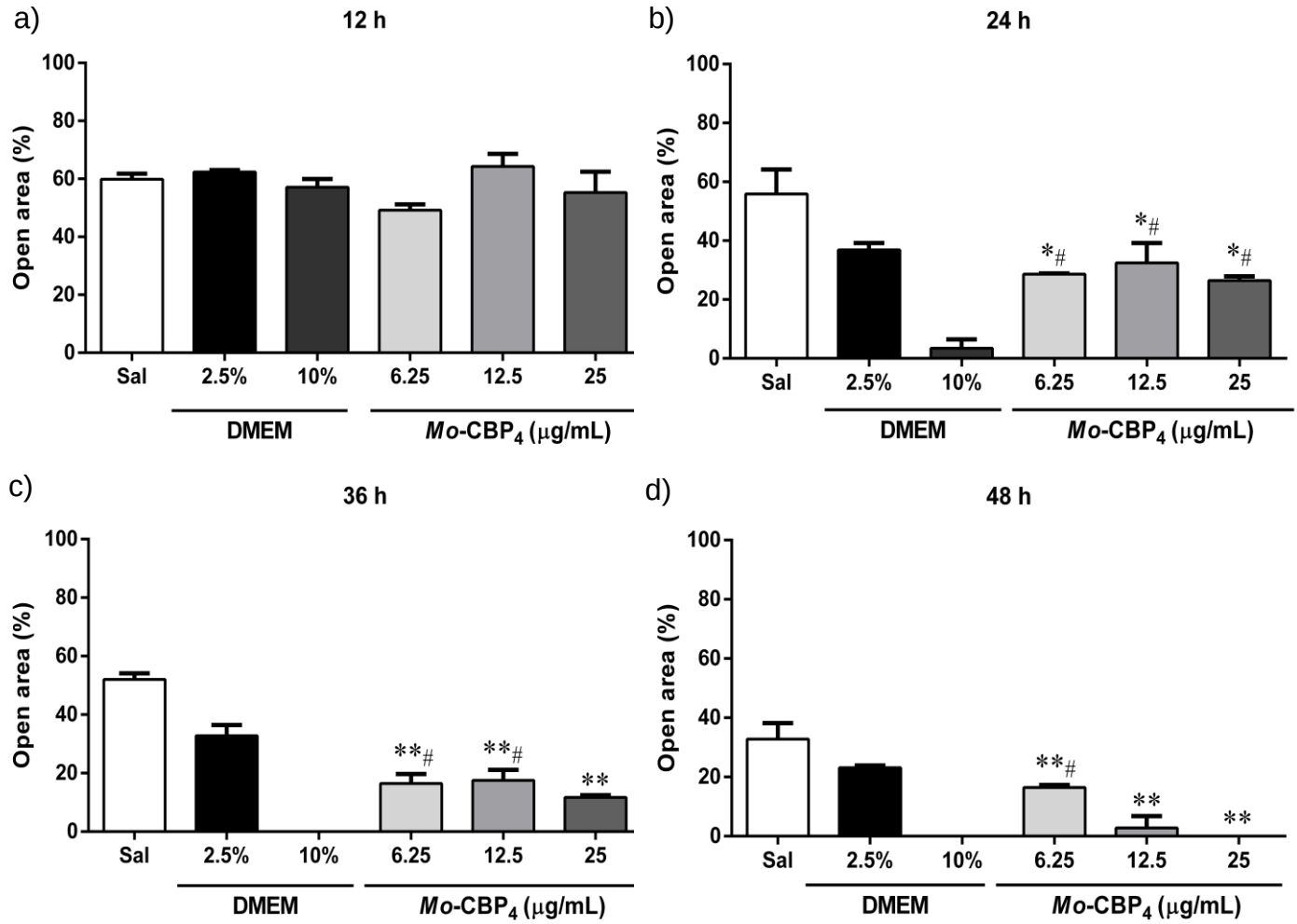

Source: prepared by the author.

Effect of *Mo*-CBP$_4$ (6.25, 12.5 and 25 µg/mL) on the proliferative and migratory activities of L929 fibroblasts in the scratch assay. The cells were incubated at 12 (a), 24 (b), 36 (c) and 48 h (d). The results were expressed as percentage of reduction in the open area (cell-free) compared to the controls and represent the means ± SD of three independent experiments. Saline and DMEM (2.5%) were used as negative controls, and DMEM (10%) as positive control. *P < 0.05 compared to saline, **P < 0.05 compared to DMEM (2.5%) and $^{\#}$P < 0.05 compared to DMEM (10%) (ANOVA followed by Bonferroni's posttest).

Figure 12 - Photomicrographsof scratch areas immediately after scratching (0 h) and 12, 24, 36 and 48 h after incubation of cells with *Mo*-CBP$_4$

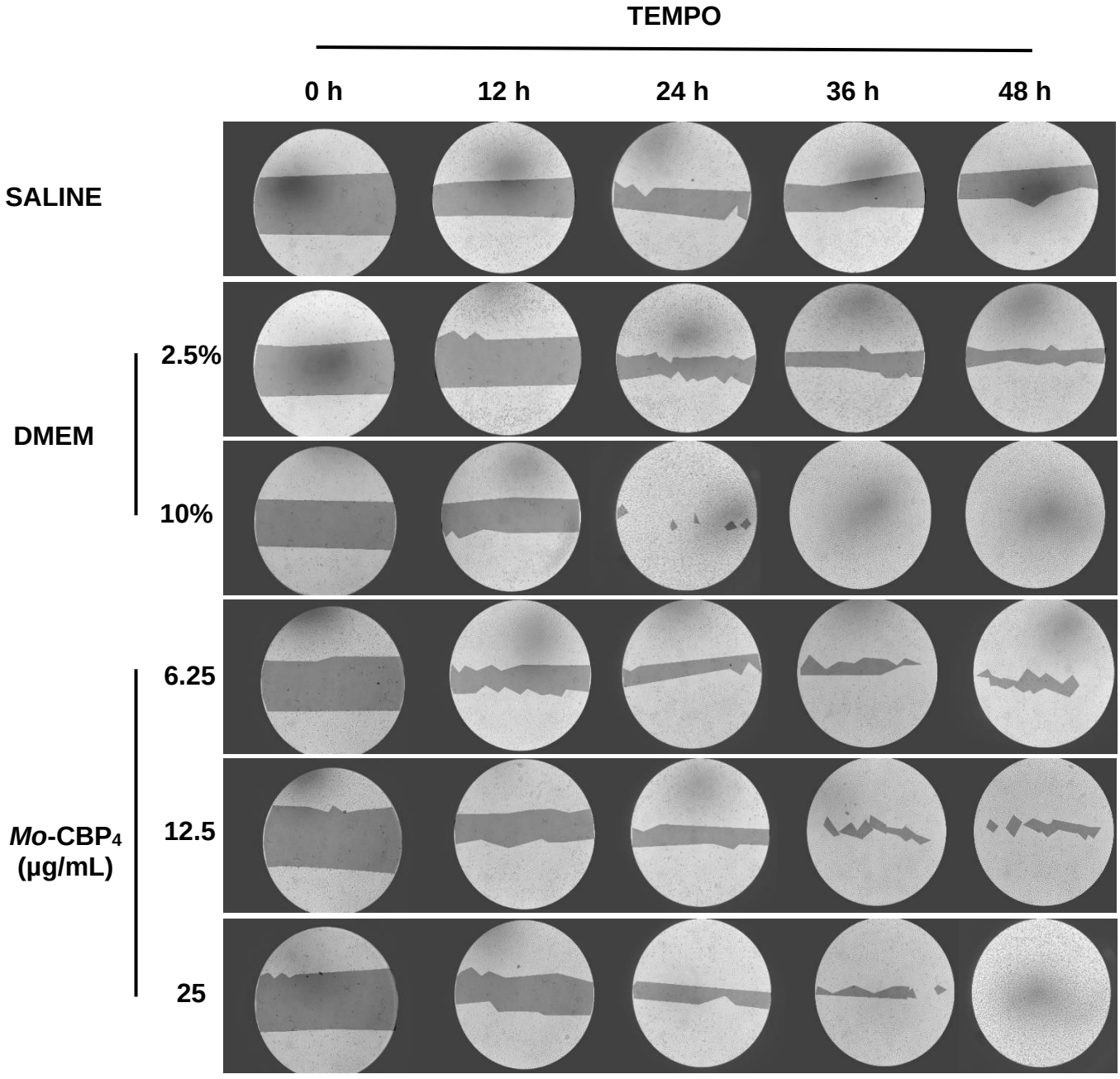

Source: prepared by the author.
Photomicrographs (200x magnification) of scratch areas immediately after scratching (0 h) and 12, 24, 36 and 48 h after incubation of cells with *Mo*-CBP$_4$ (6.25, 12.5 and 25 µg/mL) comparing to the negative (saline and 2.5% DMEM) and positive (10% DMEM) control groups. The photomicrographs were produced by the analysis of the open area (%) using the TSCRATCH® software.

6.3.2 In vivo study

6.3.2.1 Macroscopic Analyses

The measurements of the wound area in mm^2 were performed at the 2^{nd}, 5^{th}, 7^{th}, 9^{th} and 12^{th} days after surgery, in all tested groups. The results were expressed as percentage of wound area contraction (Fig.13). At the 2^{nd} and 5^{th} day of treatment with 1% and 5% PVA/M_4, no statistically significant differences were observed in relation to the Sham (with no membrane) and control (1% PVA) groups (Fig. 13a, b). From the 7^{th} day after the treatment, the results showed significant differences, relatively to the Sham and control groups. At the 7^{th} day, in the groups treated with 1% and 5% PVA/M_4, the wound contraction was around 69% and 66%, respectively, while in the SHAM and control groups, the wound contraction was around 45% and 43%, respectively (Fig. 13c). At the 9^{th} day, in the groups treated with 1% and 5% PVA/M_4, the wound contraction was around 94% and 88%, respectively, while in the SHAM and control groups, the wound contraction was around 69% (Fig. 13d). At the 12^{th} day, in the groups treated with 1% and 5% PVA/M_4, the wound closed completely, showing a contraction rate of 100%, while in the SHAM and control groups, the wound contraction was around 90% (Fig. 13e). In none of the tested days, significant differences were observed between the Sham and control groups. There were also no significant differences between the groups treated with 1% PVA/M_4 and 5% PVA/M_4, showing that the treatments were not dose dependent. Figure 14 shows images of lesions on the second, seventh and twelfth day, after the induction of the wounds, in mice submitted to different treatments. It is clear the acceleration of wound contraction in mice treated with 1% and 5% PVA/M_4.

Figure 13 - Wound contraction (%) measurements at the 2nd, 5th, 7th, 9th and 12th days after induction.

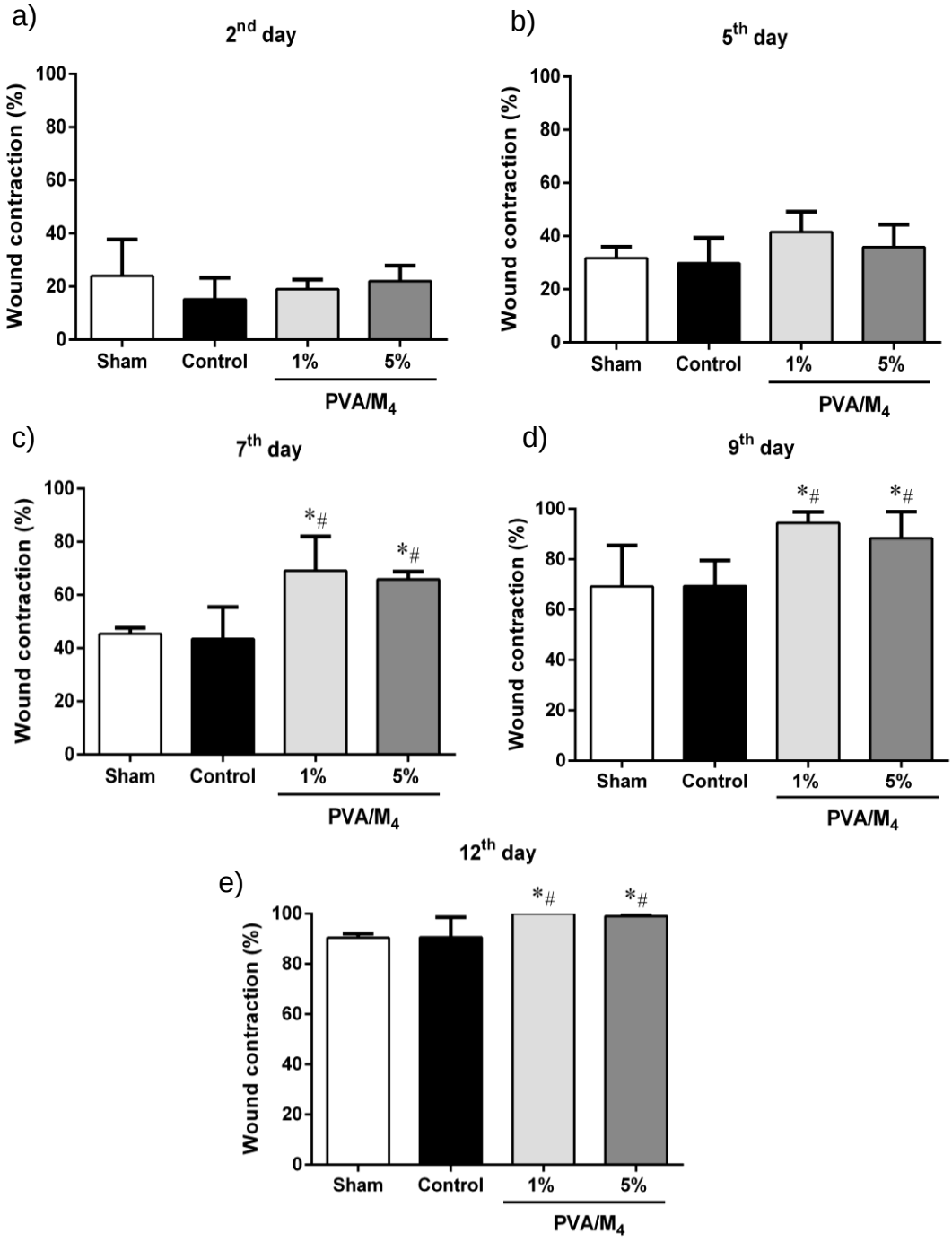

Source: prepared by the author.
The results were expressed as percentage of wound contraction compared to the controls and represent the means ± SD of three independent experiments (n=10). The Sham group was formed by animals subjected only to surgical procedures and the Control group by animals treated with 1% polyvinyl alcohol membrane. *P < 0.05 compared to Sham and #P < 0.05 compared to control (ANOVA followed by Bonferroni's posttest).

Figure 14 - Images obtained from excision wound model in four different animals (one per group) with 2, 7 and 12 days of treatment.

Source: prepared by the author.
Images obtained from excision wound model in four different animals (one per group) with 2, 7 and 12 days of treatment. The 1% and 5% PVA/M_4 groups were treated with biomembranes containing the *Mo*-CBP_4 protein. The Sham group was formed by animals subjected only to surgical procedures and the control group by animals treated with 1% polyvinyl alcohol membrane without the protein.

6.3.2.2 Histopathological Analyses

The control group (1% PVA), at the 2nd and 7th day, also presented lesions in the epidermis and superficial dermis and showed a proliferation of the inflammatory cells. At the 12th day, it presented presented epidermis with beginning of reepithelization, proliferation of the superficial dermis, neovascularization and inflammatory infiltrate. The 1% PVA/M_4 group, at the 2nd day, presented discontinuous epidermis, keratinocyte proliferation and inflammatory infiltrate. At the 7th day, it showed an already reconstituted but thin epidermis and proliferation of inflammatory cells. Already on the 12th day, this group presented a normal epidermis and dermis. The 5% PVA/M_4 group, at the 2nd day, showed a crust on the epidermis and a slight proliferation of inflammatory cells. At the 7th day, it presented thin epidermis and intact dermis with a greater amount of extracellular matrix and inflammatory infiltrate. Already on the 12th day, this group presented an intact epidermis and dermis (Fig. 15).

6.3.2.3 Measurement of cytokines

The cytokine measurements were performed on tissue samples after 2 days of treatment with PVA/M_4 biomembranes. Regarding TNF-α levels, the group treated with 1% PVA/M_4 showed an increase (509 pg/mg) when compared to the control group (304 pg/mg). This group also presentes a higher content of IL-1β (2,354 pg/mg) in comparison with control group (1,697 pg/mg).In relation to the levels of IL-10, the group treated with 1% PVA/M_4 presented 1,113 pg/mg of tissue, whereas the control group presented 359 pg/mg of tissue. The treatments with the PVA/M_4 biomembranes did not behave in a dose dependent manner, since the groups treated with 5% PVA/M_4 did not present significant differences in relation to the control groups of none of the dosed cytokines (Fig. 16).

Figure 15 - Representative photomicrographs (HE staining, x100) of the control (1% PVA), 1% PVA/M_4 and 5% PVA/M_4 groups, at the 2nd, 7th and 12th days after the wound induction, showing the main macroscopic changes. The arrows indicate inflammatory infiltrate.

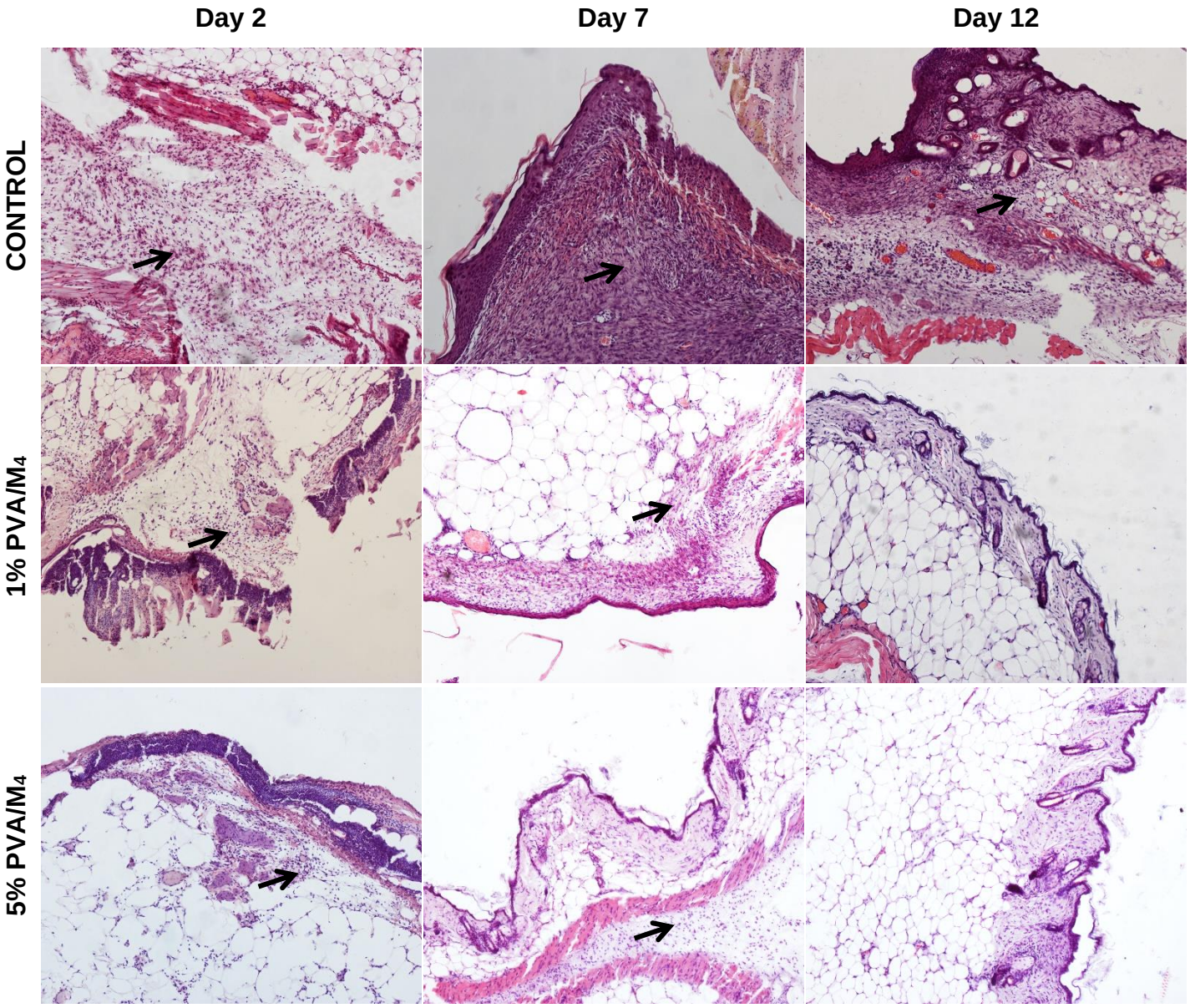

Source: prepared by the author.

Figure 16 - Effect of treatment with PVA/M_4 biomembranes on the levels of (a) TNF-α, (b) IL-1β and (c) IL-10.

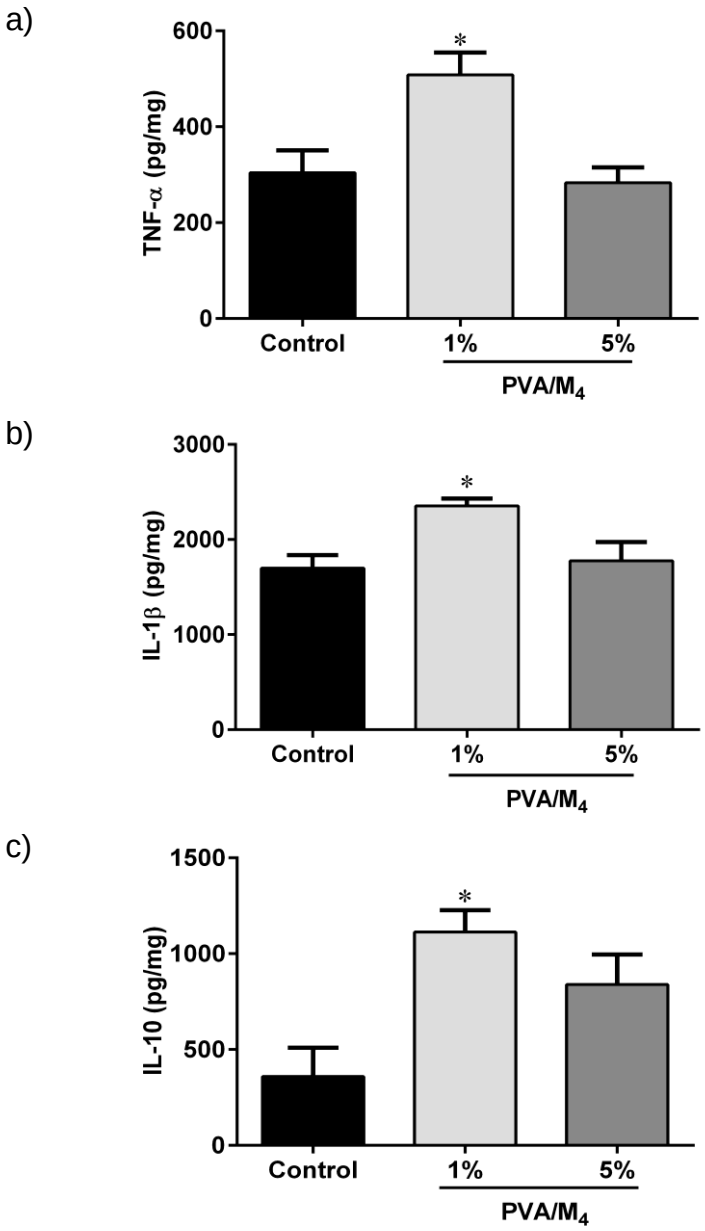

Source: prepared by the author.

The results were expressed as cytokines levels in pg per mg of tissue compared to the controls and represent the means ± SD of three independent experiments (n=6). The Control group was formed by animals treated with 1% polyvinyl alcohol membrane without the protein. *P < 0.05 compared to Control (ANOVA followed by Bonferroni's posttest). Levels of TNF-α, IL-1β and IL-10 were determined using ELISA kits on granulation tissue homogenate obtained on 2nd post-wounding day from excision wound model.

6.4 Discussion

A wound is a disrupted state of the tissue, caused by either physical, chemical, microbial, or immunological insults (MOHAMED ALI-SEYED; SIDDIQUA AYESHA, 2020). The healing process of wound is a normal biological response to the injury that occurs naturally and requires a sequence of events, including inflammation, proliferation, and migration of different cell types (BASAVRAJ NAGOBA; MILIND DAVANE, 2019; AQUINO et al., 2019). Currently, coverings with different actions and active principles can be used, however, so far there is no availability of products with promising effects, in all phases of the healing process. In this scenario, there is a need for research to develop alternative, less costly, and more effective products for the treatment of skin wounds (AZEVEDO et al., 2020). In the present study and for the first time, we showed that the *Mo*-CBP$_4$ protein isolated from *M. oleifera* seeds presents wound healing properties. This medicinal species has been object of study in our laboratory, and we recently showed that *Mo*-CBP$_4$ presents a potent anti-inflammatory and antifungal action (PEREIRA et al., 2011; LOPES et al., 2020).

One of the central requirements for the medical application of materials and devices is the determination of cytotoxicity. Cell culture systems may be especially important in testing the biocompatibility of drugs, biomaterials or treatment techniques, as they allow the direct measurement of cytotoxicity and effect on cellular growth or the determination of interactions between tissue and material. These systems include different murine cell lines, however, in this work, we used the mouse fibroblast cell line (L929 - ATCC®) as a study model. Fibroblasts are in the dermis and their main function is the maintenance of the extracellular matrix through the production of macromolecules such as collagen, glycosamine glycanes and glycoproteins (WIEGAND; HIPLER, 2008).

SRB assay determines the quantity of viable cells by estimating the total protein mass without depending on the cellular metabolic function (HOUGHTON et al., 2007; CONFORTI et al., 2008). *Mo*-CBP$_4$ did not show any toxic effect on L929 cell line at any of the concentrations tested. In contrast, proliferative effects were observed in cells. This result reveals an important property of the protein under study, since cell proliferation is provable in skin regeneration and wound healing (PREMARATHNA et al., 2019).

Several investigations show that growth factors play a crucial role in wound healing through the stimulation of angiogenesis and cellular proliferation (HORMOSI; ASSAEI; BOROUJENI, 2017). Our study demonstrated the importance of two important growth factors involved in the wound healing process: the transforming growth factor (TGF-β) and vascular endothelial growth factor (VEGF). Among the growth factors and cytokines, TGF-β has the widest spectrum of actions in wound healing. This cytokine is involved in every phase of wound repair and is released by platelets, neutrophils, macrophages, fibroblasts and migrating keratinocytes (MARGADANT; SONNENBERG, 2010). In hemostasis and inflammation phase, TGF-β recruits and activates inflammatory cells including neutrophils and macrophages, whereas in proliferative phase it organizes multiple cellular responses including reepithelialization, angiogenesis, granulation tissue formation and extracellular matrix deposition (EMC). And it also In addition, TGF-β stimulates fibroblasts to proliferate and differentiate into myofibroblasts that partake in wound contraction in the remodeling phase (PENN; GROBBELAAR; ROLFE, 2012; WANG et al., 2013; MAZUMDAR et al., 2021). In the case of VEGF, a cytokine produced by numerous cell types such as keratinocytes, macrophages, and fibroblasts, one of its main roles in wound healing is in stimulation of angiogenesis. Wound healing angiogenesis involves multiple steps including vasodilation, basement membrane degradation, endothelial cell migration, and endothelial cell proliferation. VEGF also showed effects on epithelialization and collagen deposition (BAO et al., 2010; LI et al., 2021). Recently it was reported that Hesperidin, a plant flavonoid, was able to accelerate the wound healing process by up-regulation of TGF-β and VEGF (LI et al., 2021). In the present work, we observed that *Mo*-CBP$_4$ was able to stimulate an increase in the levels of these growth factors in the L929 fibroblast culture supernatant, therefore being very favorable to the healing process.

One of the main points for the wound healing process is the proliferation and migration of epithelial cells including fibroblasts. To understand these mechanisms, in this study we investigated the effects of *Mo*-CBP$_4$ on fibroblasts proliferation and migration in culture medium. For this, we use the scratch assay, widely used in the scientific community. Although these tests are unable to mimic all factors involved in complex wound healing processes, they are considered a valuable *in vitro* tool to obtain initial information on the potential for wound healing. Our findings demonstrated that *Mo*-CBP$_4$ promotes a significant stimulatory effect on fibroblast

proliferation and migration, which possibly contributes to the cutaneous wound healing process. As seen earlier, fibroblasts play a crucial role in the wound healing process by reducing the wound size and producing ECM components (HADDADI; TAMRI; JOONI, 2019; PREMARATHNA et al., 2019; SCHERER et al., 2019; TASIĆ-KOSTOV et al., 2019).

The *in vitro* tests carried out on fibroblasts demonstrated the healing potential of *Mo*-CBP$_4$. The next step of the work was to evaluate the action of the protein in an *in vivo* model through the induction of excisional wounds in mice. The main processes related to wound healing were initially described using animal models, which have provided valuable insights into the principles of wound management (GRADA; MERVIS; FALANGA, 2018). The excisional wound model involves significant loss of skin and subcutaneous tissue and allows monitoring of the healing process based on the rate of wound contraction (DAVIDSON, 1998; RAMOS et al., 2016; PEREIRA et al., 2016). The integrity of the skin is essential to provide a protective barrier between the external and internal environment. When suffering any type of injury, the healing process must be started quickly to restore its integrity, reducing the risk of infection (SABOL et al., 2012). The success of any medication used to treat wounds depends on its ability to cause immediate wound closure. Rapid healing is characterized with faster contraction (JOSHI et al., 2016). As a vehicle for application of *Mo*-CBP$_4$ in animals, Poly(vinyl alcohol) (PVA) biomembranes were produced. PVA is a semi-crystalline synthetic polymer which is easily obtained and has a relatively low cost of production. Because it is hydrophilicity, non-toxic, good chemical resistance, biocompatible and biodegradable with excellent film forming properties, PVA has been widely studied for medical and biomedical applications (STACHOWIAK; KOWALONEK, KOZLOWSKA, 2020). Several studies demonstrate the applicability of the PVA-based biomaterials in drug and biomolecule delivery system and wound healing applications. (FIGUEIREDO et al., 2014; RAMOS et al., 2016; CRUZ et al., 2019; SEQUEIRA et al., 2019).

Our results showed that membranes incorporated with *Mo*-CBP$_4$ (PVA/M$_4$) significantly increased the rate of wound contraction when compared to control groups. Thus, PVA/M$_4$ provided a faster evolution of the contraction of the lesion, reducing the risk of infection and accelerating the other stages of healing. Wound contraction can be defined as the centripetal movement of the edges of a full thickness wound to facilitate closure of the defect. Wound contraction is therefore an indicator of re-

epithelialization, granulation, angiogenesis, fibroblast proliferation, keratinocyte differentiation, and proliferation (BOAKYE et al., 2018).

In order to validate the experimental results histopathological examination was also carried out in the tissue sections of the wound area. In histopathological tests, several stages of wound healing processes (inflammation, proliferation, and remodeling) were observed within the experimental groups. Our histological findings showed reappearance of the skin structure with distinct layers of dermis and epidermis in the treated groups. In comparison to the control group that presented a delay in the wound healing process, the treated groups showed a faster remodeling. Factors such as the formation, alignment and contraction of the extracellular matrix molecules determine the integrity of the tissue. The efficiency of reorganization of ECM molecules is critically in determining the extent of wound healing and re-establishment of tissue strength (YARISWAMY et al., 2013). Histopathological examination also showed that PVA/M_4 was able to decrease the inflammatory reaction in the wound area, showing that the infiltration of inflammatory cells was reduced. Previous studies have shown that the inflammatory response is initially required for wound healing, however if the inflammatory response is elongated or exacerbated, it leads to a delay in the subsequent phases of proper wound healing and scar formation. Inhibition of the inflammatory process has been reported to facilitate wound healing (NGUYEN et al., 2017; SUI et al., 2020).

The inflammatory phase involves the secretion of various inflammatory mediators, such as cytokines that regulate wound healing through cell proliferation, neutrophil chemotaxis and connective tissue formation. The persistent high levels of these mediators are responsible for the failure to close the wound (KUBO et al., 2014; PEREIRA et al., 2016). Studies suggest that the control of inflammation linked to the appropriate wound healing process is related to the balance of pro- and anti-inflammatory cytokines in the injury environment (PERANTEAU et al., 2008; KUBO et al., 2014). Based on that, we measured the inflammatory mediators TNF-α, IL-1β and IL-10 in tissue samples with two days of treatment, a period that corresponds to the transition between the inflammatory and the proliferative phase. Treatment with 1% PVA/M_4 was able to increase both levels of TNF-α and IL-1β (pro-inflammatory cytokines) and of IL-10 (anti-inflammatory cytokine) compared to the control group. TNF-α and IL-1β play roles in the inducing of inflammation and neutrophils chemotaxis during the inflammatory phase, and in angiogenesis, immunosuppression and

production of chemotactic factors for macrophages at the late proliferative phase in the healing of a skin wound. However, excessive levels of pro-inflammatory cytokines have been reported to impair the wound healing process. The anti-inflammatory cytokine IL-10 is produced to prevent excessive inflammation during the healing of a skin wound and has already been suggested in the literature as a cytokine antagonist of pro-inflammatory cytokines (KUBO et al., 2014; JU et al., 2016). IL-10 has been reported to inhibit the migration of inflammatory cells, including monocytes, neutrophils and macrophages for injury sites (PERANTEAU et al., 2008). These results corroborate previous findings of *Mo*-CBP$_4$ that showed anti-inflammatory activity. In an experimental model of abdominal contortion, induced by acetic acid, *Mo*-CBP$_4$, at a dose of 10 mg/kg, was able to inhibit 98.9% (intraperitoneally) and 52.9% (orally) the number of abdominal contortions in mice. In addition, *Mo*-CBP$_4$ inhibited the accumulation of leukocytes in the peritoneal cavity (PEREIRA et al., 2011).

Our findings show that the profiles of cytokine production levels stimulated by treatment with 1% PVA/M$_4$ can modulate the balance between pro- and anti-inflammatory reactions during the course of wound healing in vivo.

6.5 Conclusion

This study demonstrated that *Mo*-CBP$_4$ was able to promote wound healing by inhibiting inflammatory reactions, stimulating the proliferation and differentiation of fibroblasts, and stimulating angiogenesis. These effects can be attributed to the modulation of inflammatory cytokines, including TNF-α, IL-1β and IL-10, and growth factor TGF-β and VEGF. Consequently, *Mo*-CBP$_4$ may be applicable for the treatment of wound healing.

7 CONCLUSÃO

Os dados apresentados por este trabalho mostram de forma inédita as estruturas primária e terciária de *Mo*-CBP$_4$, uma lectina ligante à quitina isolada de sementes de *M. oleifera*. Estudos de docking molecular mostraram que *Mo*-CBP$_4$ é capaz de se ligar ao GlcNAc, o que pode contribuir para a atividade anti-inflamatória apresentada pela proteína que foi capaz de diminuir a migração de neutrófilos e modular citocinas em modelo de peritonite. Em modelo de ferida cutânea excisional, a proteína também foi capaz de modular citocinas inflamatórias, além de promover a proliferação e diferenciação de fibroblastos e a indução de fatores de crescimento em cultura celular. Esses dados demonstram o potencial de *Mo*-CBP$_4$ como um promissor composto natural a ser utilizado no tratamento de cicatrização de feridas cutâneas.

REFERÊNCIAS

ABDUL-NASIR-DEEN, A. et al. Anti-inflammatory and wound healing properties of methanol leaf extract of *Physalis angulata* L. **South African Journal of Botany**, v. 133, p. 124-131, 2020.

ABRANTES, V.E.F. et al. Molecular Modeling of Lectin-Like Protein from *Acacia farnesiana* Reveals a Possible Anti-Inflammatory Mechanism in Carrageenan-Induced Inflammation. **BioMed Research International**, v. 2013, p.1-9, 2013, https://doi.org/10.1155/2013/253483.

ADAMS, P. D. et al. PHENIX: a comprehensive Python-based system for macromolecular structure solution. **Acta Crystallographica**, v. 66, p. 213-221, 2010, https://doi.org/10.1107/S0907444909052925.

AFONINE, P. V. et al. Towards automated crystallographic structure refinement with phenix. refine. **Acta Crystallographica**, v. 68, p. 352-367, 2012, https://doi.org/10.1107/S0907444912001308.

AGYARE, C. et al. An ethnopharmacological survey and in vitro confirmation of ethnopharmacological use of medicinal plants used for wound healing in Bosomtwi-Atwima-Kwanwoma area, Ghana. **Journal of Ethnopharmacology**, v. 125, p. 393-403, 2009.

AGYARE, C. *et al.* Review: African medicinal plants with wound healing properties. **Journal of Ethnopharmacology,** v. 177, p. 85-100, 2016.

ALBERTINI, B. *et al.* Novel multifunctional platforms for potential treatment of cutaneous wounds: Development and in vitro characterization. **International Journal of Pharmaceutics,** v. 440, p. 238– 249, 2013.

ALENCAR, N. M. N. et al. An anti-inflammatory lectin from *Luetzelburgia auriculata* seeds inhibits adhesion and rolling of leukocytes and modulates histamine and PGE2 action in acute inflammation models. **Inflammation Research**, v. 59, p. 245-254, 2010, https://doi.org/10.1007/s00011-009-0092-9.

ALENCAR, N. M. N. *et al*. Leguminous lectins as tools for studying the role of sugar residues in leukocyte recruitment. **Mediators of Inflammation**, v. 8, p. 107-113, 1999.

ALENCAR, N. M. N. *et al*. The galactose-binding lectin from *Vatairea macrocarpa* seeds induces in vivo neutrophil migration by indirect mechanism. **International Journal of Biochemistry and Cell Biology,** v. 35, p. 1674-1681, 2003.

ALENCAR, N. M. N. *et al*. *Vatairea macrocarpa* (Leguminosae) lectin activates cultured macrophages to release chemotactic mediators. **Naunyn-Schmiedeberg's Archives of Pharmacology**, v. 374, p. 275-282, 2007.

ALI-SEYED, M.; AYESHA, S. *Calotropis* - A multi-potential plant to humankind: Special focus on its wound healing efficacy. **Biocatalysis and Agricultural Biotechnology**, v. 28, p. 1-10, 2020.

ANWAR, F. *et al. Moringa oleifera*: A Food Plant with Multiple Medicinal Uses. **Phytotherapy research,** v. 21, p. 17-25, 2007.

AQUINO, P. E. A. et al. The Wound Healing Property of N-Methyl-(2S,4R)-trans-4-Hydroxy-L-Proline from *Sideroxylon obtusifolium* is Related to its Anti-Inflammatory and Antioxidant Actions. **Journal of Evidence-Based Integrative Medicine**, v. 24, p. 1-11, 2019.

ARAGÃO, D. P. et al. The anti-inflammatory and antinociceptive activity of albumins from *Crotalaria retusa* seeds. **Biomedicine and Pharmacotherapy,** v. 93, p. 536–542, 2017, https://doi.org/10.1016/j.biopha.2017.06.078.

ASADULLAH, K.; STERRY, W.; VOLK, H. D. Interleukin-10 therapy—review of a new approach. **Pharmacological Reviews**, v. 55, p. 241–269, 2003, https://doi.org/10.1124/pr.55.2.4.

AZEVEDO, L. P. et al. Healing potential of *Caiman yacare* (Daudin, 1802) visceral fat oil. **Wound Medicine**, v. 31, p. 1-8, 2020.

BAO, P. et al. The Role of Vascular Endothelial Growth Factor in Wound Healing. **Journal of Surgical Research**, v. 153, p. 347-358, 2009.

BARREIROS, V.C. *et al.* Morphological and morphometric analyses of crushed sciatic nerves after application of a purified protein from natural latex and hyaluronic acid hydrogel. **Growth Factors**, v. 32, p. 164–170, 2014.

BATISTA, A.B. *et al.* New Insights into the Structure and Mode of Action of *Mo*-CBP$_3$, an Antifungal Chitin-Binding Protein of *Moringa oleifera* Seeds. **Plos one**, v. 9, 2014.

BERTHELOT, K.; PERUCH, F.; LECOMTE, S. Highlights on *Hevea brasiliensis* (pro) hevein proteins. **Biochimie**, v. 127, p. 258-270, 2016, https://doi.org/10.1016/j.biochi.2016.06.006.

BEZERRA, M.G.B. **Atividade anti-inflamatória, antinociceptiva e pro-cicatrizante de uma nova lectina purificada do muco do caramujo *Achatina fulica* BOWDITH 1822.** Tese (Doutorado em Bioquímica) – Universidade Federal do Ceará, 2015.

BEZERRA, M.J.B. *et al*. Crystal Structure of *Dioclea violaceae* lectin and a comparative study of vasorelaxant properties with *Dioclea rostrata* lectin. **The International Journal of Biochemistry & Cell Biology,** v. 45(4), p. 807-815, 2013.

BHATNAGAR, M. *et al.* Hemostatic, antibacterial biopolymers from *Acacia arabica* (Lam.) Willd. and *Moringa oleifera* (Lam.) as potential wound dressing materials. **Indian Journal of Experimental Biology,** v. 51, p. 804-810, 2013.

BHUTIA, S.K. et al. Plant lectins in cancer therapeutics: Targeting apoptosis and autophagy-dependent cell death. **Pharmacological Research**, v. 144, p. 8–18, 2019.

BOAKYE, Y. D. et al. Assessment of Wound-Healing Properties of Medicinal Plants: The Case of *Phyllanthus muellerianus.* **Frontiers in Pharmacology**, v. 9, p. 1-12, 2018.

BRADLEY, P. P. et al. Measurement of cutaneous inflammation: estimation of neutrophil content with an enzyme marker. **Journal of Investigative Dermatology**, v. 78, p. 206-209, 1982, https://doi.org/10.1111/1523-1747.ep12506462.

CARDOSO, J. F. et al. Effects of cigarette smoke in mice wound healing is strain dependent. **Toxicologic Pathology**, v. 35, p. 890–896, 2007.

CARNEIRO, R.F. et al. Elucidation of the primary structure and molecular modeling of *Parkia pendula* lectin and i*n vitro* evaluation of the leishmanicidal activity. **Process Biochemistry**, v. 101, p. 1–10, 2021.

CARVALHO, A.S. *et al*. Purification, characterization and antibacterial potential of a lectin isolated from *Apuleia leiocarpa* seeds. **International Journal of Biological Macromolecules**, v. 75, p.402-408, 2015.

CAVADA, B.S. et al. A review of *Vicieae* lectins studies: End of the book or a story in the writing? **International Journal of Biological Macromolecules**, v. 181, p. 1104–1123, 2021.

CHARUNGCHITRAK, S. *et al*. Antifungal and antibacterial activities of lectin from the seeds of *Archidendron jiringa* Nielsen. **Food Chemistry**, v. 126, p.1025-1032, 2011.

CHEN, V. B. et al. MolProbity: all-atom structure validation for macromolecular crystallography. **Acta Crystallographica**, v. 66, p. 12-21, 2010, https://doi.org/10.1107/S0907444909042073.

CHETTRI, D.; BORO, M.; SARKAR, L.; VERMA, A.K. Lectins: Biological significance to biotechnological application. **Carbohydrate research**, v. 506, 2021.

CHIN, C. et al. Development and formulation of *Moringa oleifera* standardised leaf extract film dressing for wound healing application. **Journal of Ethnopharmacology**, v. 212, p. 188-199, 2018.

CHOPRA, R. N. **Indigenous Drugs of India**, v.1, p.364, 1993.

CHUANG, P.H. *et al.* Anti-fungal activity of crude extracts and essential oil of *Moringa oleifera* Lam. **Bioresource Technology**, v. 98, p. 232-236, 2007.

COELHO, R. C. **Análise toxicológica e avaliação da estabilidade de uma proteína ligante à quitina isolada de sementes de *Moringa oleifera* como perspectiva de sua utilização como um biofármaco**. Monografia (Bacharelado em Biologia) - Universidade Federal do Ceará, 2013.

COLLABORATIVE COMPUTATIONAL PROJECT, Number 4. The CCP4 suite: programs for protein crystallography. **Acta Crystallographica Section D: Biological Crystallography**, v. 50, p. 760–763, 1994.

CONFORTI, F. et al. Antiproliferative activity against human tumor cell lines and toxicity test on Mediterranean dietary plants. **Food and Chemical Toxicology**, v. 46, p. 3325-3332, 2008.

CORIOLANO, M. C. *et al. Parkia pendula* seed Lectin: Potential Use to Treat Cutaneous Wounds in Healthy and Immunocompromised Mice. **Biotechnology and Applied Biochemistry,** v. 172, p. 2682-2693, 2014.

CRETELLA, A. B. M. et al. Expanding the anti-inflammatory potential of *Moringa oleifera*: topical effect of seed oil on skin inflammation and hyperproliferation. **Journal of Ethnopharmacology**, v. 254, p. 1-12, 2020.

CRUZ, M. V. et al. Immobilization of antimicrobial trypsin inhibitors onto cashew gum polysaccharide/PVA films. **International Journal of Biological Macromolecules**, v. 127, p. 433-439, 2019.

CUNHA, J. M. et al. Cytokine mediated inflammatory hyperalgesia limited by interleukin-1 receptor antagonist. **British Journal of Pharmacology**, v. 130, p. 1418–1424, 2000, https://doi.org/10.1038/sj.bjp.0703434.

CUNHA, T. M. et al. A cascade of cytokines mediates mechanical inflammatory hypernociception in mice. **Proceedings of the National Academy of Sciences**, v. 102, p. 1755–1760, 2005, https://doi.org/10.1073/pnas.0409225102.

CUNHA, T. M. et al. Role of cytokines in mediating mechanical hypernociception in a model of delayed-type hypersensitivity in mice. **European Journal of Pain,** v. 12, p. 1059–1068, 2008, https://doi.org/10.1016/j.ejpain.2008.02.003.

CUNHA, T. M. et al. TNF-α and IL-1β mediate inflammatory hypernociception in mice triggered by B1 but not B2 kinin receptor. **European Journal of Pharmacology,** v. 573, p. 221-229, 2007, https://doi.org/10.1016/j.ejphar.2007.07.007.

DAVIDSON, J. M. Animal models for wound repair. **Archives of Dermatological Research**, v. 290, p. 1-11, 1998.

DELANO, W.; LAM, J. PyMOL: A communications tool for computational models. **Abstracts of Papers of the American Chemical Society**, v. 230, p.1371–1372, 2005.

DELATORRE, P. *et al.* Interactions between indole-3-acetic acid (IAA) with a lectin from *Canavalia maritima* seeds reveal a new function for lectins in plant physiology. **Biochimie**, v. 95(9), p. 1697-1703, 2013.

DEV, S. K. et al. Antimicrobial, anti-inflammatory and wound healing activity of polyherbal formulation. **Biomedicine & Pharmacotherapy**, v. 111, p. 555-567, 2019.

DOHERTY, N. S. et al. Intraperitoneal injection of zymosan in mice induces pain, inflammation and the synthesis of peptidoleukotrienes and prostaglandin E2. **Prostaglandins**, v. 30, p. 769-89, 1985, https://doi.org/10.1016/0090-6980(85)90006-1.

ECHOLS, N. et al. Graphical tools for macromolecular crystallography in PHENIX. **Journal of Applied Crystallography**, v. 45, p. 581-586, 2012, https://doi.org/10.1107/S0021889812017293.

EMSLEY, P. et al. Features and Development of Coot. **Acta Crystallographica**, v. 66, p. 486-501, 2010, https://doi.org/10.1107/S0907444910007493.

EZZAT, S. M.; CHOUCRY, M. A.; KANDIL, Z. A. Antibacterial, antioxidant, and topical anti-inflammatory activities of *Bergia ammannioides*: A wound-healing plant. **Pharmaceutical Biology**, v. 54, p. 215-224, 2016.

FELDMANN, M.; PUSEY, C. D. Is There a Role for TNF-α in Anti-Neutrophil Cytoplasmic Antibody–Associated Vasculitis? Lessons from Other Chronic Inflammatory Diseases**. Journal of the American Society of Nephrology**, v.17, p. 1243–1252, 2006, https://doi.org/10.1681/ASN.2005121359.

FERREIRA, P.M.P. *et al. Moringa oleifera*: bioactive compounds and nutritional potential. **Revista de Nutrição**, v. 21, p. 431-437, 2008.

FERREIRA, R. S. *et al.* Coagulant and antibacterial activities of the water-soluble seed lectin from *Moringa oleifera.* **Letters in Applied Microbiology,** v. 53, p. 186-192, 2011.

FIGUEIREDO J. G. et al. Pharmacological analysis of the neutrophil migration induced by *Dioclea rostrata* lectin: Involvement of cytokines and nitric oxide. **Toxicon**, v. 54, p. 736-744, 2009, https://doi.org/10.1016/j.toxicon.2009.05.037.

FIGUEIREDO, I. S. T. et al. Efficacy of a membrane composed of polyvinyl alcohol as a vehicle for releasing of wound healing proteins belonging to latex of *Calotropis procera*. **Process Biochemistry**, v. 49, p. 512-519, 2014.

FRANCHIN, M.; CUNHA, M. G.; DENNY, C. et al. Geopropolis from *Melipona scutellaris* decreases the mechanical inflammatory hypernociception by inhibiting the production of IL-1β and TNF-α. **Journal of Ethnopharmacology**, v. 143, p.709–715, 2012, https://doi.org/10.1016/j.jep.2012.07.040.

FREIRE, J. E. et al. *Mo*-CBP$_3$, an antifungal chitin binding protein from *Moringa oleifera* seeds, is a member of the 2S albumin family. **PLoS One,** v. 10, p. e0119871, 2015, https://doi.org/10.1371/journal.pone.0119871.

FRIEDMAN, A. Wound healing: from basic science to clinical practice and beyond. **Journal of Drugs in Dermatology**, v. 10, p. 427–433, 2011.

GEBÄCK, T. et al. TScratch: a novel and simple software tool for automated analysis of mono-layer wound healing assays. **Short Technical Reports**, v. 46, p. 265-274, 2009.

GEORGE, T.T. et al. *Moringa oleifera* through the years: a bibliometric analysis of scientific research (2000-2020). **South African Journal of Botany,** v. 141, p. 12–24, 2021.

GHAZARIAN, H. *et al*. A glycobiology review: Carbohydrates, lectins and implications in cancer therapeutics. **Acta Histochemical**, v. 113, p. 236–247, 2011

GIFONI, J.M. *et al*. A Novel Chitin-Binding Protein from *Moringa oleifera* Seed with Potential for Plant Disease Control. **Peptide Science**, v. 98, p. 406-415, 2012.

GRADA, A.; MERVIS, J.; FALANGA, V. Research Techniques Made Simple: Animal Models of Wound Healing. **Journal of Investigative Dermatology**, v. 138, p. 2095-2105, 2018.

HADDADI, R.; TAMRI, P.; JOONI, F. J. *In vitro* wound healing activity of *Scrophularia striata* hydroalcoholic extract. **South African Journal of Botany**, v. 121, p. 505-509, 2019.

HALL, L. W.; CLARKE, K. W. **Veterinary anaesthesia**, 9. ed, 1991.

HARATA, K.; MURAKI, M. Crystal Structures of *Urtica dioica* Agglutinin and its Complex with Tri-N-acetylchitotriose. **Journal of Molecular Biology**, v. 297, p. 673-681, 2000, https://doi.org/10.1006/jmbi.2000.3594.

HIREMATH, K.Y. A lectin with anti-microbial and anti proliferative activities from *Lantana camara*, a medicinal plant. **Protein Expression and Purification**, v. 170, 2020.

HORMOSI, M.; ASSAEI, R.; BOROUJENI, M. B. The effect of aloe vera on the expression of wound healing factors (TGFβ1 and bFGF) in mouse embryonic fibroblast cell: In vitro study. **Biomedicine & Pharmacotherapy**, v. 88, p. 610-616, 2017.

HOUGHTON, P. et al. The sulphorhodamine (SRB) assay and other approaches to testing plant extracts and derived compounds for activities related to reputed anticancer activity. **Methods**, v. 42, p. 377-387, 2007.

HUKKERI, V. I. et al. Antipyretic and Wound Healing Activities of *Moringa oleifera* Lam. in Rats. **Indian Journal of Pharmaceutical Sciences**, v. 68, p. 124-126, 2006.

JOSHI, A. et al. Systematic investigation of ethanolic extract from *Leea macrophylla*: Implications in wound healing. **Journal of Ethnopharmacology,** v. 191, p. 95-106, 2016.

JU, H. W. et al. Wound healing effect of electrospun silk fibroin nanomatrix in burn-model. International **Journal of Biological Macromolecules**, v. 85, p. 29-39, 2016.

KABSCH, W. XDS. **Acta Crystallographica Section D: Biological Crystallography**, v. 66, p. 125–132, 2010.

KATRE, U. V. *et al*. Structure-activity relationship of a hemagglutinin from *Moringa oleifera* seeds, **International Journal of Biological Macromolecules**, v. 42, p. 203-207, 2008.

KIM, D.; KU, B.; CHOI, E. Se-methylselenocysteine stimulates migration and antioxidant response in HaCaT keratinocytes: Implications for wound healing. **Journal of Trace Elements in Medicine and Biology**, v. 58, p. 1-7, 2020.

KLAFKE, G.B. *et al*. Assessment of plant lectin antifungal potential against yeasts of major importance in medical mycology. **Mycopathology**. v. 175, p.147-51, 2013.

KOLACZKOWSKA, E.; SELJELID, R.; PLYTYCZ, B. Role of mast cells in zymosan-induced peritoneal inflammation in Balb/c and mast cell-deficient WBB6F1 mice. **Journal of Leukocyte Biology**, v. 69, p. 33-42, 2001, https://doi.org/10.1189/jlb.69.1.33.

KRISHNAN, P. The scientific study of herbal wound healing therapies: current state of play. **Curr. Anaesth. Crit.,** v. 17, p. 21–27, 2006.

KUBO, H. et al. Temporal expression of wound healing-related genes in skin burn injury. **Legal Medicine**, v. 16, p. 8-13, 2014.

LI, D. et al. MicroRNA-132 enhances transition from inflammation to proliferation during wound healing. **The Journal of Clinical Investigation**, v. 125, p. 3008-3026, 2015.

LI, D. F. et al. Crystal structure of mabinlin II: a novel structural type of sweet proteins and the main structural basis for its sweetness. **Journal of Structural Biology**, v. 162, p. 50 – 62, 2008, https://doi.org/10.1016/j.jsb.2007.12.007.

LI, H. et al. Repair function of essential oil from *Crocodylus Siamensis* (Schneider, 1801) on the burn wound healing via up-regulated growth factor expression and anti-inflammatory effect. **Journal of Ethnopharmacology**, v. 264, p. 1-12, 2021.

LIS, H.; SHARON, N. Lectins: carbohydrate-specific proteins that mediate cellular recognition. **Chemical Reviews**, v.98, p.637-674, 1998.

LIU, Z. *et al*. Could plant lectins become promising anti-tumour drugs for causing autophagic cell death? **Cell Proliferation**, v. 46, p. 509–515, 2013.

LOPES, T. D. P. L. et al. *Mo*-CBP$_4$, a purified chitin-binding protein from *Moringa oleifera* seeds, is a potent antidermatophytic protein: In vitro mechanisms of action, in vivo effect against infection, and clinical application as a hydrogel for skin infection. **International Journal of Biological Macromolecules**, v. 149, p. 432-442, 2020.

LOPES, T.D.P. **Potencial antidermatofítico de *Mo*-CBP$_4$, uma proteína ligante à quitina de sementes de *Moringa oleifera*.** Dissertação (Mestrado em Bioquímica) – Universidade Federal do Ceará, 2016.

LORIS, R. Principles of structures of animal and plant lectins. **Biochimica et Biophysica Acta**, v. 1572, p. 198-208, 2002.

LOWE, J. B. Glycan-dependent leukocyte adhesion and recruitment in inflammation. **Current Opinion in Cell Biology,** v. 15, p. 531–538, 2003.

LUZ, L. A. *et al*. Structural characterization of coagulant *Moringa oleifera* Lectin and its effect on hemostatic parameters. **International Journal of Biological Macromolecules**, v. 58, p. 31-36, 2013.

MACEDO, M. L. R.; OLIVEIRA, C. F. R.; OLIVEIRA, C. T. Insecticidal Activity of Plant Lectins and Potential Application in Crop Protection. **Molecules**, v. 20, p. 2014-2033, 2015.

MARGADANT, C.; SONNENBERG, A. Integrin–TGF-β crosstalk in fibrosis, cancer and wound healing. **European Molecular Biology Organization**, v. 11, p. 97-105, 2010.

MATHIEU, D.; LINKE, J.C.; WATTEL, F. Non-healing wounds. **Hand book on Hyperbaric Medicine**, p. 401–427, 2006.

MATTHEWS, B. W. Solvent content of protein crystals. **Journal of Molecular Biology**, v. 33, p. 491–497, 1968, https://doi.org/10.1016/0022-2836(68)90205-2.

MAZUMDAR, S. et al. Evaluation of wound healing activity of ethanol extract of *Annona reticulata* L. leaf both in vitro and in diabetic mice model. **Journal of Traditional and Complementary Medicine**, v. 11, p. 27-37, 2021.

MBIKAY, M. Therapeutic potential of *Moringa oleifera* leaves in chronic hyperglycemia and dyslipidemia: a review. **Frontiers in pharmacology**, v. 3, 2012.

MCCOY, A. J. et al. Phaser crystallographic software. **Journal of Applied Crystallography**, v. 40, p. 658-674, 2007, https://doi.org/10.1107/S0021889807021206.

MISHRA, A. et al. Structure-function and application of plant lectins in disease biology and immunity. **Food and Chemical Toxicology**, v. 134, 2019.

MOHAMEDY, E.; ABDALLA, A.M. Evaluation of antifungal activity of *Moringa oleifera* extracts as natural fungicide against some plant pathogenic fungi *in-vitro*. **Journal of Agricultural Technology**, v. 10, p. 963-982, 2014.

MOREIRA, R. A.; PERRONE, J. C. Purification and partial characterization of a lectin from *Phaseolus vulgaris*. **Plant Physiology**, v. 59, p. 783-787, 1977, https://doi.org/10.1104/pp.59.5.783.

MORRIS, G. M. et al. AutoDock4 and AutoDockTools4: Automated Docking with Selective Receptor Flexibility. **Journal of Computational Chemistry**, v. 30, p. 2785-2791, 2009, https://doi.org/10.1002/jcc.21256.

MORTAZ, E. et al. Update on neutrophil function in severe inflammation. **Frontiers in Immunology,** v. 9, p.1–14, 2018, https://doi.org/10.3389/fimmu.2018.02171.

MOTA, M. R. L. *et al*. Modulation of acute inflammation by a chitin-binding lectin from *Araucaria angustifolia* seeds via mast cells. **Naunyn-Schmiedeberg's Archives of Pharmacology**, v. 374, p. 1-10, 2006.

MOURA, L.I.F. *et al*. Recent advances on the development of wound dressings for diabetic foot ulcer treatment—A review. **Acta Biomaterialia**, v. 9, p. 7093–7114, 2013.

MUHAMMAD, A. A. et al. Evaluation of wound healing properties of bioactive aqueous fraction from *Moringa oleifera* Lam on experimentally induced diabetic animal model. **Drug Design, Development and Therapy**, v. 10, p. 1715-1730, 2016.

MURAKAMI, K. *et al.* Hydrogel blends of chitin/chitosan, fucoidan and alginate as healing-impaired wound dressings. **Biomaterials,** v. 31, p. 83–90, 2010.

MURDOCK, L. L.; SHADE, R. E. Lectins and protease inhibitors as plant defense against insects. **Journal of Agricultural and Food Chemistry**, v. 50, p. 6605–6611, 2002.

NAGOBA, B.; DAVANE, M. Studies on wound healing potential of topical herbal formulations- do we need to strengthen study protocol? **Journal of Ayurveda and Integrative Medicine**, v. 10, p. 316-318, 2019.

NAPIMOGA, M.H. *et al. Lonchocarpus sericeus* lectin decreases leukocyte migration and mechanical hypernociception by inhibiting cytokine and chemokines production. **International Immunopharmacology,** v. 7, p. 824-35, 2007.

NATHAN, C. Neutrophils and immunity: challenges and opportunities. **Nature Reviews Immunology,** v. 6, p. 173–182, 2006.

NÉMETH, T.; SPERANDIO, M.; MÓCSAI, A. Neutrophils as emerging therapeutic targets. **Nature Reviews Drug Discovery**, v. 19, p. 253–275, 2020, https://doi.org/10.1038/s41573-019-0054-z.

NGUYEN, V. et al. Anti-inflammatory and wound healing activities of calophyllolide isolated from *Calophyllum inophyllum* Linn. **Plos one**, v. 12, p. 1-16, 2017.

NOVA, E. et al. Potential of *Moringa oleifera* to improve glucose control for the prevention of diabetes and related metabolic alterations: A systematic review of animal and human studies. **Nutrients**, v. 12, p.1–28, 2020.

NUNES, B.S. et al. Lectin extracted from *Canavalia grandiflora* seeds presents potential anti-inflammatory and analgesic effects. **Naunyn-Schmiedeberg's Archives of Pharmacology,** v. 379, p. 609-16, 2009, https://doi.org/10.1007/s00210-009-0397-9.

OLIVEIRA, C.M.B. *et al*. Citocinas e Dor. **Revista Brasileira de Anestesiologia**, v. 61, p. 255-265, 2011.

PADAYACHEE, B.; BAIJNATH, H. An updated comprehensive review of the medicinal, phytochemical and pharmacological properties of *Moringa oleifera.* **South African Journal of Botany**, v. 129, p. 304-316, 2020.

PAIVA, P. M. G. *et al.* Effect of lectins from *Opuntia ficus indica* cladodes and *Moringa oleifera* seeds on survival of *Nasutitermes corniger*. **International Biodeterioration & Biodegradation,** v. 65, p. 982-989, 2011.

PANTOJA-UCEDA, D. et al. Solution structure of allergenic 2S albumins. **Plant Food Allergens**, v. 30, p. 919-924, 2002, https://doi.org/10.1042/bst0300919.

PENN, J. W.; GROBBELAAR, A. O.; ROLFE, K. J. The role of the TGF-β family in wound healing, burns and scarring: a review. **International Journal of Burns and Trauma**, v. 2, p.18-28, 2012.

PERANTEAU, W. H. et al. IL-10 Overexpression Decreases Inflammatory Mediators and Promotes Regenerative Healing in an Adult Model of Scar Formation. **Journal of Investigative Dermatology**, v. 128, p. 1852-1860, 2008.

PERCIVAL, N.J. Classification of wounds and their management. **Surgery,** v. 20, p. 114–117, 2002.

PEREIRA, C. A. *et al.* Hemaglutinina de folhas de mandioca (*Manihot esculenta Crantz*): purificação parcial e toxicidade. **Ciência e Agrotecnologia,** v. 32(3), p. 900-907, 2008.

PEREIRA, L. P. *et al.* Modulator effect of a polysaccharide-rich extract from *Caesalpinia ferrea* stem barks in rat cutaneous wound healing: Role of TNF-α, IL-1β, NO, TGF-β. **Journal of Ethnopharmacology,** v. 187, p. 213–223, 2016.

PEREIRA, M. L. et al. Purification of a Chitin-Binding Protein from *Moringa oleifera* Seeds with Potential to Relieve Pain and Inflammation. **Protein & Peptide Letters**, v. 18, p. 1078-1085, 2011.

PEREIRA, M.L. **Aspectos estruturais, farmacológicos e toxicológicos de *Mo*-CBP$_4$, uma proteína ligante à quitina de *Moringa oleifera* com atividade anti-inflamatória e antinociceptiva via oral.** Tese (Doutorado em Bioquímica) – Universidade Federal do Ceará, 2014.

PEUMANS, W. J.; VAN DAMME, E. J. M. Lectins as plant defense proteins. **Plant Physiology**, v. 109, p. 347-352, 1995, https://doi.org/10.1104/pp.109.2.347.

POPOOLA, J.O. et al. A systematic review of pharmacological activities and safety of *Moringa oleifera*. **Journal of Herbmed Pharmacology**, v. 9, p. 174–190, 2020.

PRATA, M. B. et al. Uso tópico do açúcar em feridas cutâneas: estudo experimental em ratos. **Acta cirúrgica brasileira,** v. 3, p. 43-48, 1988.

PREMARATHNA, A. M. et al. Wound healing properties of aqueous extracts of *Sargassum illicifolium*: An in vitro assay. **Wound Medicine**, v. 24, p. 1-7, 2019.

RAMACHANDRAN, C.; PETER, K.V.; GOPALAKRISHNAN, P.K. Drumstick (*Moringa oleifera*): A Multipurpose Indian Vegetable. **Economic Botany**, v. 34, p. 276-283, 1980.

RAMOS, M. V. et al. Wound healing modulation by a latex protein-containing polyvinyl alcohol biomembrane. **Naunyn-Schmiedeberg's Archives of Pharmacology**, v. 389, p. 747-756, 2016.

RAMZI, S.C.; VINAY, K.; STANLEY, R. Pathologic Basis of Diseases, **WB Saunders Company**, p.86, 1994.

RÄSÄNEM, K.; VAHERI, A. Proliferation and motility of HaCaT keratinocyte derivatives is enhanced by fibroblast nemosis. **Experimental cell research**, v. 316, p. 1739-1747, 2010.

RAWAT, S. *et al.* Wound healing Agents from Medicinal Plants: A Review. **Asian Pacific Journal of Tropical Biomedicine,** p. 1910-1917, 2012.

RIBEIRO, A.E.A.S. et al. Inhibitory effects of *Morus nigra* L. (Moraceae) against local paw edema and mechanical hypernociception induced by *Bothrops jararacussu* snake venom in mice. **Biomedicine and Pharmacotherapy**, v. 111, p. 1046–1056, 2019, https://doi.org/10.1016/j.biopha.2019.01.011.

ROSALES, C. Neutrophil: A cell with many roles in inflammation or several cell types? **Frontiers in Physiology**, v. 9, p.1–17, 2018, https://doi.org/10.3389/fphys.2018.00113.

ROY, A. *et al*. Binding of insecticidal lectin *Colocasia esculenta* tuber agglutinin (CEA) to midgut receptors of *Bemisia tabaci* and *Lipaphis erysimi* provides clues to its insecticidal potential. **Proteomics**, v. 14, p. 1646-1659, 2014.

SABOL, F. et al. Immunohistological changes in skin wounds during the early periods of healing in a rat model. **Veterinarni Medicina**, v. 57, p. 77-82, 2012.

SACHAN, D.; JAIN, S.K.; SINGH, N. *In-vitro* & *in-vivo* efficacy of *Moringa oleifera* plant constituents in urolithiasis as antilithiatic drug. **International Journal of Pharmaceutical Sciences and Research**, v. 2, p. 1638-1644, 2011.

SAMPIETRO, A. R. *et al.* An N-acetylglucosamine oligomer binding agglutinin (lectin) from ripe *Cyphomandra betacea* Sendt. Fruits. **Plant Science,** v. 160, p. 659-667, 2001.

SANTI-GADELHA, T. *et al*. Purification and biological effects of *Araucaria angustifolia* (Araucariaceae) seeds lectin. **Biochemical and Biophysical Research Communications**, v. 350, p. 1050-1055, 2006.

SANTI-GADELHA, T. et al. Purification of a PHA-Like chitin-binding protein from *Acacia farnesiana* seeds: a time-dependent oligomerization protein. **Applied Biochemistry and Biotechnology**, v. 150, p. 97–111, 2008, https://doi.org/10.1007/s12010-008-8144-0.

SANTOS, A. F. S. *et al.* Detection of water soluble lectin and antioxidant component from *Moringa oleifera* seeds. **Water Research**, v. 39, p. 975–980, 2005.

SANTOS, A. F. S. *et al*. Isolation of a seed coagulant *Moringa oleifera* lectin. **Process Biochemistry**, v. 44, p. 504-508, 2009.

SANTOS, L.M.N. et al. Anti-Candida activity of the water-soluble lectin from *Moringa oleifera* seeds (WSMoL). **Journal of Medical Mycology**, v. 31, 2021.

SARAIVA, M.; VIEIRA, P.; O'GARRA, A. Biology and therapeutic potential of

interleukin-10. **Journal of Experimental Medicine**, v. 217, p. 1–19, 2019, https://doi.org/10.1084/jem_20190418.

SAUL, S. A. *et al.* Crystal structure of *Urtica dioica* agglutinin, a superantigen presented by MHC molecules of class I and class II. **Structure**, v. 8, p. 593–603, 2000.

SCHERER, M. M. C. et al. Wound healing activity of terpinolene and α-phellandrene by attenuating inflammation and oxidative stress in vitro. **Journal of Tissue Viability**, v. 28, p. 94-99, 2019.

SEQUEIRA, R. S. et al. Development of a poly(vinyl alcohol)/lysine electrospun membrane-based drug delivery system for improved skin regeneration. **International Journal of Pharmaceutics**, v. 570, p. 1-14, 2019.

SHARON, N.; LIS, H. History of lectins: from hemagglutinins to biological recognition molecules. **Glycobiology,** v. 14, p. 53-62, 2004.

SILVA NETO, J.X. **Purificação, caracterização bioquímica e atividade contra *Candida* spp. de uma nova proteína ligante à quitina de sementes de *Moringa oleifera* LAM**. Dissertação (Mestrado em Bioquímica) – Universidade Federal do Ceará, 2015.

SINGH, H.; SARATHI, S.P. Insight of Lectins – A review. **International Journal of Scientific & Engineering Research,** v. 3, 2012.

SINGH, S.; YOUNG, A.; MCNAUGHT, C. The physiology of wound healing. **Surgery**, v. 35, 473-477, 2017.

SIVARANJANI, V.; PHILOMINATHAN, P. Synthesize of Titanium dioxide nanoparticles using *Moringa oleifera* leaves and evaluation of wound healing activity. **Wound Medicine,** v. 12, p. 1-5, 2016.

SOUSA, B.L. *et al.* High-resolution Structure of a new Tn antigen-binding lectin from *Vatairea macrocarpa* and a comparative analysis of Tn-binding legume lectins. **The International Journal of Biochemistry & Cell Biology,** v. 59, p. 103-110, 2015.

STACHOWIAK, N.; KOWALONEK, J.; KOZLOWSKA, J. Effect of plasticizer and surfactant on the properties of poly(vinyl alcohol)/chitosan films. International **Journal of Biological Macromolecules**, v. 164, p. 2100-2107, 2020.

STRODTBECK, F. Physiology of Wound Healing. **Newborn and Infant Nursing Reviews**, v. 1, 2001.

SUI, H. et al. A wheat germ-derived peptide YDWPGGRN facilitates skin wound healing processes. **Biochemical and Biophysical Research Communications**, v. 524, p. 943-950, 2020.

SULTANI, M. et al. Anti-inflammatory cytokines: Important immunoregulatory factors contributing to chemotherapy-induced gastrointestinal mucositis. **Chemotherapy Research and Practice**, v. 2012, p. 1-11, 2012, https://doi.org/10.1155/2012/490804.

SÜNTAR, I.P. *et al.* Wound healing acceleration effect of endemic Ononis species growing in Turkey. **Journal of Ethnopharmacology**, v.135, p. 63–70, 2011.

TALREJA, T. Screening of crude extract of flavonoids of *Moringa oleifera* against bacterial and fungal pathogen. **Journal of Phytology**, v. 11, p. 31-35, 2010.

TASIĆ-KOSTOV, M. et al. Towards a modern approach to traditional use: *in vitro* and *in vivo* evaluation of *Alchemilla vulgaris* L. gel wound healing potential. **Journal of Ethnopharmacology**, v. 238, p. 1-12, 2019.

THAKUR, R. *et al*. Practices in Wound Healing Studies of Plants. **Evid-Based Compl. Alt**., 2011.

TRINDADE, M. B. *et al.* Structural characterization of novel chitin-binding lectins from the genus *Artocarpus* and their antifungal activity. **Biochimica et Biophysica Acta**, v. 1764, p. 146-152, 2006.

TSANEVA, M.; VAN DAMME, E.J.M. 130 years of Plant Lectin Research. **Glycoconjugate journal**, v. 37, 2020.

ULLAH, A. et al. Crystal structure of mature 2S albumin from *Moringa oleifera* seeds. Biochem. **Biochemical and Biophysical Research Communications**, v. 468, p. 365–371, 2015, https://doi.org/10.1016/j.bbrc.2015.10.087.

USTUNER, O. et al. In Vitro Evaluation of Antioxidant, Anti-Inflammatory, Antimicrobial and Wound Healing Potential of *Thymus Sipyleus* Boiss. Subsp. *Rosulans* (Borbas) *Jalas*. **Molecules**, v. 24, p. 3353-3374, 2019.

VAN DAMME, E. J. M. *et al*. Plant lectins: a composite of several distinct families of structurally and evolutionary related proteins with diverse biological role. **Critical Reviews in Plant Sciences**, v. 17, p. 575–692, 1998.

VAN HOLLE, S.; VAN DAMME, E. J. M. Distribution and Evolution of the Lectin Family in Soybean (Glycine max). **Molecules**, v. 20, p. 2868-2891, 2015, https://doi.org/10.3390/molecules20022868.

VESTWEBER, D.; BLANKS, J. Mechanisms that regulate the function of the selectins and their ligands. **Physiological Reviews**, v. 79, p. 181-213, 1999.

WANG, D. et al. Green tea polyphenols mitigate the plant lectins-induced liver inflammation and immunological reaction in C57BL/6 mice via NLRP3 and Nrf2 signaling pathways. **Food and Chemical Toxicology**, v. 144, 2020.

WANG, X. et al. Effects of TRAP-1-Like Protein (TLP) Gene on Collagen Synthesis Induced by TGF-b/Smad Signaling in Human Dermal Fibroblasts. **Plos one**, v. 8, p. 1-8, 2013.

WIEGAND, C.; HIPLER, U. Methods for the measurement of cell and tissue compatibility including tissue regeneration processes. **GMS Krankenhaushygiene Interdisziplinär**, v. 3, p. 1-9, 2008.

YAN, Q. *et al.* Characterization of a novel monomeric lectin (AML) from *Astragalus membranaceus* with anti-proliferative activity. **Food chemistry,** v. 122(3), p. 589-595, 2010.

YAO, Q. *et al.* A new chitin-binding lectin from rhizome of *Setcreasea purpurea* with antifungal, antiviral and apoptosis-inducing activities. **Process Biochemistry**, v. 45, p. 1477-1485, 2010.

YARISWAMY, M. et al. Topical application of serine proteases from *Wrightia tinctoria* R. Br. (Apocyanaceae) latex augments healing of experimentally induced excision wound in mice. **Journal of Ethnopharmacology,** v. 149, p. 377-383, 2013.

ZANETTI, G. D. **Lectina dos rizomas de *Arundo donax* L.: purificação, caracterização, propriedades, imuno-histoquímica e separação das isoformas**. Tese (Doutorado em Bioquímica) – Universidade Federal do Rio Grande do Sul, 2007.